

1 **Drumlin sedimentology in a hard-bed, lowland setting, Connemara,**
2 **western Ireland: implications for subglacial bedform generation in**
3 **areas of sparse till cover**

4 David J.A. Evans, David H. Roberts and Colm Ó Cofaigh

5 Department of Geography, Durham University, South Road, Durham, DH1 3LE, UK

6

7 **Abstract**

8 Cores of coastal drumlins in Connemara contain stratified diamictos that interdigitate with gravelly
9 clinofolds and finer grained rhythmites. The diamictos are interpreted as subaqueous mud apron
10 deposits delivered by subglacial till advection to continuously failing subaqueous ice-contact fans, whose
11 strata were being syn-depositionally over-steepened by glacitectonic deformation. The localized nature
12 of the stratified sediments reflects the emergence of subglacial deforming tills and meltwater deposits
13 in a glaciallacustrine environment to produce interdigitated mass flow diamictos and grounding line
14 fans/wedges. These depo-centres became glacitectonized and subglacially streamlined during glacier
15 overriding and hence regional drumlin sedimentology reflects the varying degrees of inheritance of pre-
16 existing glacial deposits and suggests that drumlin production relates more to the position of
17 localised sediment accumulations at the glacier bed than full depth till deformation processes (e.g.
18 instability mechanisms) within the same drumlin field. Till cored drumlins give way down ice to
19 stratified cored drumlins with till caps and then to stratified drumlins. This zonation is compatible with
20 the increased lateral variability in drumlin composition that would arise from the occurrence of linear
21 assemblages of glacialfluvial (esker) and subaqueous (grounding line) sediments in an otherwise marginal-
22 thickening till sheet.

23

24 Key words: drumlins; sedimentology; subaqueous fans; glacitectonics; subglacial

25

26 **1. Introduction**

27 The drumlins of western Ireland have been crucial to attempts at reconstructing the palaeoglaciology of
28 the last British-Irish Ice Sheet (Orme 1967; Synge 1968; Warren 1992; Greenwood & Clark 2008, 2009a,
29 b) as well as assessments of subglacial bedform genesis (McCabe & Dardis 1989, 1994; Dardis & Hanvey
30 1994). With respect to the latter, glacial geomorphologists have long understood that drumlins contain a

31 wide variety of sediments and structures rather than largely homogenous subglacial till, although till
32 cores apparently dominate drumlin sedimentology (see Stokes et al. 2011 and references therein) and
33 this has been central to recent advances in identifying a universal drumlin formation model related to
34 instabilities in subglacial deforming media (Hindmarsh 1998a, b; Fowler 2000; Schoof 2007; Dunlop et al.
35 2008; Stokes et al. 2013). Nevertheless, stratified drumlin cores can predominate in some locations and
36 potentially provide insights into the sedimentological origins of glacially streamlined terrain. Stratified
37 cores were central to the subglacial megaflood explanation of drumlins and flutings presented by Shaw
38 (1983; see also Shaw & Kvill 1984; Shaw et al. 1989, 2000), wherein the cores were first explained as the
39 infills of fluvially scoured cavities on the glacier sole and later additionally explained as fluvially eroded
40 remnants of pre-existing sediment. In Galway Bay, the stratified cores of drumlins are interpreted by
41 McCabe and Dardis (1989) as pre-existing subaqueous (glacimarine) sediments deposited proximal to
42 the margins of floating glacier ice and then overrun, streamlined and capped with till. This is in contrast
43 to a wider regional assessment of stratified Irish drumlins that regards stratified contents as the
44 products of lee-side stratification sequences, whereby downglacier-dipping, sorted sediments on the lee
45 side of drumlins are thought to be deposited in water-filled cavities contemporaneous with drumlin
46 streamlining (e.g. Dardis et al. 1984; Hanvey 1987; Dardis & Hanvey 1994; McCabe & Dardis 1994; Knight
47 2014). Upper till carapaces in such settings are related to subglacial shearing, which modifies or
48 streamlines the cavity fill.

49
50 Previous studies of drumlins in western Ireland (McCabe & Dardis 1989, 1994; Knight 2014) have
51 highlighted some site-specific characteristics that need to be assimilated into the search for universal
52 models of subglacial bedform genesis. These include entirely stratified cores, often with only very thin
53 till carapaces, and widely-spaced distribution patterns on an otherwise areally-scoured bedrock surface
54 in lowland terrain. The significance of these characteristics needs to be addressed through the
55 assessment of a wider range of coastal lowland drumlins, with a view to analyzing the importance of
56 relative sea level changes, glacialacustrine sedimentation and subglacial cavity filling in the evolution of
57 subglacial bedform cores (cf. Dardis & McCabe 1983, 1987; McCabe et al. 1984, 1987; Dardis 1985,
58 1987; McCabe & Dardis 1989; Thomas & Chiverrell 2006; Ó Cofaigh et al. 2008, 2011; Evans et al. 2012).
59 The coincidence of stratified drumlin cores and coastal lowland terrain potentially represents the
60 product of drumlin generation at subglacial sticky spots, the locations of which are controlled by pre-
61 existing stratified depo-centres (Boulton 1987) that originally accumulated near glacier grounding lines
62 and were connected to esker networks located inland. In this paper, this hypothesis is tested by

63 expanding the initial research of McCabe and Dardis (1989) in Galway Bay to cover the drumlins of
64 western Connemara, where a variety of drumlin core types lying on a predominantly hard subglacial bed
65 can be investigated.

66

67 **2. Study area and methods**

68 Connemara forms the northwestern highlands and bedrock coastal lowlands of County Galway, western
69 Ireland (Fig. 1a). The glacial streamlining of the lowland areas comprises elongate bedrock ridges (roches
70 moutonnées, rock drumlins and whalebacks) and sediment-cored drumlins, all indicating a predominant
71 east to west palaeo-ice sheet flow (Charlesworth 1929; Orme 1967; Synge 1968; McCabe & Dardis 1989,
72 1994; Knight 2014). This study concentrates on some spatially dispersed sediment-cored drumlins
73 overlying an expansive area of glacially scoured bedrock (Fig. 1b). Three sites were chosen for intensive
74 sedimentological analysis within Mannin Bay and Ballyconneely Bay (cf. Knight 2014) based upon
75 excellent natural coastal cliff exposures and a road cut.

76

77 The glacial geomorphology of the study area (Fig. 1b) was mapped using a combination of the
78 topographic data on the Irish Ordnance Survey 1:50,000 scale map sheet 44 and aerial imagery available
79 on Google Earth (Fig. 1), checked and verified by field observations. This facilitated an assessment of the
80 spatial distribution of sediment-cored drumlins on an otherwise aerially scoured bedrock terrain.

81

82 Sedimentological and stratigraphical investigations were undertaken on the drumlin exposures and are
83 recorded in scaled section sketches and vertical profile logs, in places augmented with panoramic
84 photomosaics. Information was recorded on primary sedimentary structures, bed contacts, sediment
85 body geometry, sorting and texture, and the resulting data and observations were used to characterize
86 individual lithofacies, which were classified according to the facies codes proposed by Eyles et al. (1983)
87 and Evans and Benn (2004). Palaeocurrent directions were reconstructed where bedding structures
88 indicated a direction of sediment progradation into standing water. Secondary sedimentary structures,
89 such as faults, folds and cross-cutting intrusions or clastic dykes, were also logged and used, where
90 appropriate, to measure stress directions. The orientations of structural features were depicted as great
91 circles on stereonet using the Rockworks software programme.

92

93 Clast macrofabrics were measured on samples of 50 and occasionally 30 clasts from the diamictons
94 using A axes and A/B plane dips and orientations and processed in Rockworks stereonet software and

95 depicted using Schmidt equal-area lower hemisphere projections. The macrofabrics were then analysed
96 for strength, modality and isotropy following procedures outlined by Benn (1994, 2004a), Hicock et al.
97 (1996) and Evans et al. (2007). This approach allows an assessment not only of the direction of applied
98 stress but also, in combination with other sedimentological data and observations, the genesis of the
99 deposit. Previous research on clast macrofabrics has processed both A-axis and A/B plane orientation
100 data in order to account for the variable response of passive strain markers (clasts) in deforming media
101 (matrix-supported diamictons). Specifically this acknowledges the tendency for the A-axes of elongate
102 clasts to rotate towards parallelism with the shearing direction in thicker deforming zones but to roll in
103 thinner shear zones, where A/B planes would tend to align preferentially and hence lock into the tightly
104 constrained fissile and compact structure of the diamicton (Benn 1995; Benn & Evans 1996; Evans &
105 Hiemstra 2005; Evans et al. 2006, 2007; Li et al. 2006). Hence A/B planes weaken as deforming zones
106 thicken or become more fluidal in nature.

107
108 Micromorphology of selected diamictons was assessed qualitatively and semi-quantitatively using a
109 total of 5 thin sections (each c. 50 - 75 mm in size) from Ballyconneely. Micromorphological sampling,
110 preparation and analysis followed procedures outlined by Murphy (1986), van der Meer (1993), Menzies
111 (2000), Carr (2004) and Hiemstra (2007).

112
113 Clast form analyses were undertaken on metamorphic grade rocks, including Powers roundness and
114 clast shape, following the procedures outlined in Benn (2004b). Roundness was assessed visually using
115 histogram plots and statistically by calculating an RA value (percentage of clasts in the VA and A
116 categories), an RWR value (percentage of clasts in the R and WR categories; Benn et al., 2004; Lukas et
117 al. 2013) and an average roundness value, wherein VA = 0, A = 1, SA = 2, SR = 3, R = 4, WR = 5 (cf.
118 Spedding and Evans, 2002; Evans, 2010; Evans et al. 2010). Because the RWR-index expands the
119 discriminatory power of clast form analysis, we employ it in tandem with RA values and average
120 roundness. Clast shape was analysed statistically by using clast shape triangles (Benn, 2004b) from
121 which C40 indices were derived and compared to RA, RWR and average roundness values in co-variance
122 plots following procedures outlined in Benn and Ballantyne (1994). Unequivocal deposits from which
123 control samples for clast form assessment are normally derived (i.e. screes, subglacial tills, glacialfluvial
124 gravels etc) were not available locally, so comparisons were made with datasets collected from similar
125 lithologies in glaciated terrains in New Zealand (Fig. S1; Evans et al. 2010).

126

127

128 **3. Glacial geomorphology**

129 The study area lies directly south of the Connemara Mountains, a landscape of well developed cirques
130 and other alpine glacial topography, and comprises an intermediate to low relief landscape of
131 streamlined bedrock knobs and numerous intervening ponds or lakes (Figs. 1 & 2). This landscape is
132 typical of knock and lochan topography, the product of areal scouring by ice sheet glaciation (Linton
133 1963; Sugden & John 1976; Rea & Evans 1996). Mannin and Ballyconneely bays are separated by a
134 bedrock peninsula that contains some isolated high points up to 60 m but is generally a low relief knock
135 and lochan landscape containing isolated streamlined sediment hills or drumlins up to 30 m high (Figs.
136 1b & 2). Previous reconstructions of ice sheet glaciation in this region (Synge 1968; Warren 1992; Smith
137 & Knight 2011) indicate that glacier flow radiated from a lowland-based dispersal centre located over
138 Roscommon, presumably augmented by ice flowing from the upland areas of the Connemara Mountains
139 (Twelve Pins and Maumturk Mountains), converging on outer Galway Bay to flow directly westward to
140 the continental shelf edge (Ballantyne et al., 2008; Ó Cofaigh et al. 2012). This regional ice flow pattern
141 resulted in a predominant westerly flow over the areal scour terrain of the study area.

142

143 The restricted assemblages of sediment on the areal scour terrain of the study area comprise isolated
144 drumlins which are distributed in a largely linear pattern. They are readily apparent in aerial imagery
145 due to their well vegetated surfaces and on topographic maps where the contours define their ovoid
146 morphology (Fig. 1b, c).

147

148 **4. Drumlin sedimentology**

149 4.1 North Ballyconneely Bay

150 *Description*

151 The ≤ 10 m high and 300 m long section in North Ballyconneely Bay (L 619/430; Fig. 1b) is orientated
152 parallel to the long axis of an ENE-WSW aligned drumlin with a summit at 22m OD. The architecture of
153 the bedding along most of the exposure is predominantly horizontal but the true dip is apparent at the
154 western end of the section where a large scale clinoform structure dips WNW at angles of up to 40°,
155 towards the centreline of the drumlin (Fig. 3a). Bedding dips in the same sedimentary units decline
156 towards angles of 4-14° together with more westerly dip directions at the western end of the section.
157 The clinoform bedding architecture represents significant oversteepening at the eastern end of the
158 sediment stack, indicative of incipient open fold development.

159

160 Details of the lithofacies are presented at four locations along the exposure in vertical profile logs 1-4
161 (Fig. 3b). At the eastern end of the section, logs 1 and 2 reveal vertically stacked diamictons separated
162 by discontinuous but laterally extensive lenses of stratified sediments and/or erosional contacts (Fig.
163 3b). The diamictons are predominantly matrix-supported and macroscopically massive, although locally
164 they may appear crudely laminated/fissile or contain clast-rich horizons (Fig. 4a). The stratified sediment
165 lenses are dominated by laminated silts and sands. The lowermost diamictons between logs 1 and 2 are
166 cross-cut by a sub-vertical clastic dyke which ascends from the section base through the host materials
167 for 2 m before bifurcating into a series of sub-horizontal ribbons which gradually wedge out after
168 ascending a further 1 m in a westerly direction (Fig. 3a). At the western end of the section, logs 3 and 4
169 (Fig. 3b) reveal a higher degree of stratification and based upon the WNW dip in the bedding, represent
170 the upper part of the stratigraphic sequence in the drumlin (Fig. 3). The sequence in log 3 comprises
171 interbedded diamictons and discontinuous but laterally extensive stratified sands and gravels overlying
172 rhythmically bedded silts and fine sands with dropstones (Fig. 4e). The diamictons in the lower part of
173 log 3 range from crudely to well stratified and matrix-supported. They have interbedded, gradational
174 and scoured/erosional contacts with associated stratified sediment bodies and lenses which comprise
175 laminated and horizontally bedded sands, and rhythmites with dropstones and gravel lags. The
176 diamictons also contain gravel clusters and sand/silt intraclasts. At the base of log 3, an increasingly thin
177 set of diamicton and intervening sand beds forms a gradational sequence with underlying matrix-
178 supported gravel and minor sand beds. The diamictons in the upper part of log 3 comprise massive to
179 laminated, matrix-supported lensate bodies which have been scoured and infilled by a sequence of
180 clast-supported, stratified diamictons interbedded with discontinuous sand and gravel lenses. The
181 sequence in log 4 represents the westerly-fining of the sediments in log 3 (Fig. 3), and contains the best
182 exposure of rhythmically bedded silts and fine sands with dropstones. These are conformably overlain
183 by stratified, matrix-supported diamicton, which in turn grades vertically into massive diamicton. The
184 occurrence of rhythmites in both logs 3 and 4 as well as in the area of steeply dipping beds directly to
185 the east of log 3, indicates that the lower strata in this part of the section cliff have been post-
186 depositionally steepened to produce the incipient open fold structure.

187

188 Thin section slides were prepared for a variety of sediment types at North Ballyconneely Bay with a view
189 to further elucidating former depositional processes. Sample B'Conn 4 is a macroscopically massive
190 diamicton (Dmm) from the lower unit in Log 1. (Fig. 3b). It has a clay/silt/sand matrix of very densely

191 packed, angular to sub-rounded skeletal clasts, 30-40 mm in diameter and of mixed lithologies. The
192 sample contains several plasmic fabrics with 'halos' and skelsepic fabrics as well as faint microshears and
193 a cross cutting latteseptic fabric.

194 Another partially stratified diamicton (Fig. 5a), sample B'Conn 5 is from the lower unit in Log 2 (Fig. 3b).
195 It has a silt/clay matrix with heterogeneous texture and sub-rounded skeletal grains up to 20mm in
196 diameter. It includes some intraclasts of sorted silt/clay with internal grading, occasional dropstones
197 within intraclasts and some evidence for compression and contortion of pre-existing sedimentary
198 laminae. There is also some faint evidence for secondary fluidisation, rotation and necking. Plasmic
199 fabrics include common skelsepic fabrics around skeletal clasts, common masepic fabrics and variable
200 domain textures.

201

202 Sample B'Conn 2 is from the lowest unit in Log 4. It is composed of interlaminated sands, silts and clays,
203 which comprises laminae of < 2mm – 10mm in thickness and contains angular to sub-rounded skeletal
204 clasts up to 10 mm in diameter (Fig. 5b). The laminae show abruptly alternating grain size with some
205 grading and fining upwards, as well as dropstones and some intraclast dropstones. There are also
206 alignments of silt and sand grain long axes subparallel to bedding together with evidence of secondary
207 fluidisation of laminae due to water escape/hydrofracture in the form of lens/pod structures
208 interdigitated with primary laminae. Structures include minor open folds, normal and reverse faulting,
209 low angle shear faults, minor boudinage and extension of laminae. Plasmic fabrics include unistrial
210 fabrics slightly oblique to laminae, kinking fabrics in clay laminae and skelsepic fabric around some
211 skeletal clasts. In addition there is secondary deposition of Fe on laminae contacts.

212 Sample B'Conn 3 is a partially stratified diamicton (Dms) that has a clay/silt matrix with angular to sub-
213 rounded skeletal grains, 10-20 mm in diameter. Stratification appears as partially sorted and distorted
214 clay/silt/sand laminae with occasional graded couplets and dropstones. Structures include minor reverse
215 faulting, occasional hydrofractures/water escape features through the clay laminae and slight contortion
216 or open folding. Plasmic fabrics show strong birefringence sub-parallel to the bedding, occasional
217 patches of unistrial fabric with laminae, occasional kinked fabric in clay laminae and some skelsepic
218 plasmic fabric development around skeletal clasts. However, the main matrix lacks plasmic fabric.

219

220 Sample B'Conn 6 is a crudely stratified diamicton, also from the second unit in Log 4 (Fig. 3b). It has a
221 clay/silt/sand matrix with very densely packed, angular to sub-rounded skeletal clasts, 20-30 mm in
222 diameter and of mixed lithologies. The micro-structure is chaotic and discontinuous with convoluted
223 laminae. There is no grading but there is a clear differentiation between silt/clay laminae and
224 sandy/diamictic laminae. Also visible are possible fluidisation structures (pipes and pods), Type III
225 intraclasts with internal masepic fabrics, multiple domains and possible rotational pressure shadows.
226 Plasmic fabrics reveal some matrix 'halos' and skelsepic fabrics with Type III intraclasts with internal
227 masepic fabrics and multiple domains.

228
229 Clast forms in the diamictons sampled from all four profile log locations reveal typically subglacial
230 characteristics, with the sub-angular average roundness and good preservation of striae (8-74% of
231 samples) being particularly diagnostic. The co-variance plot for RA/C40 (Fig. S2) indicates abnormally
232 high C40 indices compared to data presented by Benn and Ballantyne (1994), a trend that has been
233 identified in other studies utilizing metamorphic grade lithologies, which appear to break preferentially
234 along densely spaced joints and thereby tend not to produce blocks when subject to subglacial wear
235 (e.g. Evans et al. 2010). In such situations the employment of average roundness and C40 co-variance
236 (Fig. S2) often provides a more discriminatory tool with which to differentiate sediments according to
237 their clast transport histories (Fig. S1). However, the clast form data (Fig. S2) reveal that average
238 roundness values are relatively uniform across the range of C40 values, indicative of a strong subglacial
239 signature on all clast forms. This is reflected also in the RWR values which are all zero.

240
241 Clast macrofabrics from the diamictons and matrix-supported gravels in the North Ballyconneely Bay
242 section display a wide range of strength values but reasonably consistent orientations (Fig. 3b and Fig.
243 S3). The clast fabric shape ternary plots (Fig. S3) reveal generally stronger A-axis than A/B plane
244 orientations, the former being characterised by girdle to weak clusters (Fig. S3 left) and the latter
245 representing generally greater isotropy (Fig. S3 right). Most of the clast macrofabric dip orientations
246 display a range of alignments between southwest and northwest with weak subsidiary clusters either
247 opposite or orthogonal to those westerly directions. The strongest A-axis macrofabrics are those from
248 the matrix-supported gravels and massive, matrix-supported diamicton in Log 3 (Fig. 3b, F2 & F3) and
249 the massive, matrix-supported diamicton in Log2 (Fig. 3b, F1; Fig. S3). Although A/B plane macrofabric
250 alignments generally closely resemble those of their respective A-axes samples, only A/B plane sample

251 F2 from the Dmm in log 1 displays a significant clustering but with generally high dip angles (Figs. 3b &
252 Fig. S3 right).

253

254 *Interpretation*

255 The predominantly horizontally bedded architecture of the inter-stratified and conformable sequence of
256 diamictons and matrix-supported coarse gravels, silt and sand lenses, sand and gravel beds and lenses,
257 rhythmite beds with dropstones and gravel lags in the North Ballyconneely Bay section is interpreted as
258 a glacier-proximal subaqueous fan in which alternating gravelly and diamictic, cohesionless and cohesive
259 sediment gravity mass flows and coarse-grained suspension sedimentation dominated the depositional
260 processes (Fig. 6; cf. Rust & Romanelli 1975; Cheel & Rust 1982; Powell 1990; Benn 1996). Deep water
261 sedimentation is recorded by the widespread occurrence of laminated silts and sands and dropstones.
262 Samples B'Conn 2 and B'Conn 3 from the lower part of Log 4 clearly demonstrate primary subaqueous
263 sedimentation. The graded and ungraded laminae point predominantly to suspension rain out from
264 overflows with additional ice rafted inputs. The sandy, diamictic laminae and lenses could relate to
265 episodic inputs from sediment gravity flows with inverse grading pointing to turbulent flow and
266 kinematic sieving (Fig. 5b; Talling et al., 2012), although Knight (2014) has previously noted that the
267 lack of ripples suggests that traction current activity was limited. The crude lamination in the
268 intervening thick diamictons, which were at least in part likely to have been the product of ice-proximal
269 rain-out but more predominantly subaqueous cohesive debris flows (cf. Nemeč and Steel, 1984; Postma,
270 1986; Postma et al., 1983; Mulder and Alexander, 2001; Powell, 2003). Discontinuous lenses of silts,
271 sands, gravels, together with gravel lags, represent periods of traction current and underflow activity.
272 The proximity of a glacier input source to the depo-centre is strongly reflected in the coarse to diamictic
273 nature of the sediment sequence as well as the clear subglacial signature in the clast form data. The
274 close proximity of the grounding line could also be partially reflected within the micromorphological
275 signature in samples B'Conn 4 and 5 from Logs 1 and 2. Sample B'Conn 4 from the base of the sequence
276 exhibits skelsepic and lattesepic plasmic fabrics as well as microshears, all of which have been used
277 previously to infer intergranular rotation and discrete brittle shear in a subglacial environment (van der
278 Meer 1993; Carr 2004; Hiemstra, 2007). However, some of these features could result from mass flow
279 processes (Lachniet et al 1999, 2001; Phillips 2006) and indeed such a mechanism is supported by
280 sample B'Conn 5 where primary subaqueous structures (e.g. sedimentary grading; dropstones) have
281 been subject to minor compression and contortion with secondary liquefaction, fluidisation, rotation
282 and necking. Additional small scale features noted in the other thin section samples, such as boudinage,

283 kinked plasmic fabrics and high birefringence subparallel to laminae contact boundaries, also support a
284 mass flow origin with secondary dewatering and consolidation (Phillips 2006). The increasingly gravelly
285 nature of the sedimentary sequence towards the west end of the exposure, which is also
286 stratigraphically the uppermost part of the sequence, records more distal and later stages of shallow
287 subaqueous fan sedimentation. The significant increase in bedding dip angle immediately to the east of
288 Log 3 (Fig. 3a), because it is not associated with any lateral changes in individual bed thickness,
289 particularly in finer-grained rhythmically bedded units, is interpreted as the product of post-, or at least
290 late, syn-depositional open folding. Beds dipping at angles as high as 40° towards the northwest are a
291 product of over-steepening through ice front compression of the fan when the ice margin flowing from
292 the east-southeast advanced into the sediment pile. A scoured contact or erosional unconformity at the
293 top of the sequence around Log 3 indicates that subaqueous scour and fan sedimentation continued
294 over the fold structure after its construction. It is likely that glacier snout advance into a shallow, debris
295 flow-dominated ice-contact fan resulted in the steepening of the sedimentary sequence which was then
296 partially scoured and overlain by gravelly clinoforms (Fig. 6). Evidence for minor compression (kinking
297 and open folds; normal and reverse faulting; low angle shear faults) and fluidization in samples B'Conn
298 2, 3 and 6 could potentially relate to proglacial compression of the sediment pile at the western end of
299 the section (Fig 5b). Minor boudinage plus skelsepic and unistrial fabrics in samples B'Conn 3 and
300 B'Conn 6 could relate to overriding of the sediment pile with increasing deformation up section.
301 However, we re-iterate here that although such microscale features have in the past been associated
302 with subglacial sediment deformation (e.g. van der Meer, 1993; Carr 2004; Hiemstra, 2007), an
303 emerging body of research is increasingly documenting them associated with sediment gravity flow
304 deposits (Lachniet et al 1999, 2001; Phillips 2006); both interpretations are consistent with the
305 macroscale sedimentological evidence presented more broadly from the outcrop.

306
307 We suggest that localized fissility within the diamictons, especially towards the top of the eastern part of
308 the exposure, may have been imparted by shearing induced by the passage of glacier ice after
309 subaqueous sediment deposition. In support of this interpretation, the clast A-axis and A/B plane
310 macrofabrics taken from this fissile zone reveal a strong NE-SW orientation (Log 1, F3), which is aligned
311 with drumlin long axis orientation in the study area. The girdle-like nature of all the remaining A-axis
312 macrofabrics may reflect deposition by shallow gradient mass flows or rain out, with weak south-
313 westerly to north-westerly alignments reflecting the dominant mass flow directions driven by sediment-
314 laden meltwater debouching from the nearby glacier snout portal. The consistently higher dip angles

315 and more isotropic nature of the A/B plane macrofabrics likely reflects the tendency for clast A-axes to
316 become preferentially aligned in more fluidized flows and for the more slab-like clasts to rotate more
317 freely in the low strain environment of both cohesive and cohesionless subaqueous sediment gravity
318 flows.

319

320 The sub-vertical clastic dyke and associated bifurcating series of sub-horizontal ribbons which cross-cut
321 the lowermost diamictos between logs 1 and 2, are interpreted as a hydrofracture fill linked to burst-
322 out structures, created by the release of pressurized groundwater (Rijsdijk et al. 1999). The gradual
323 ascent of the sub-horizontal ribbons in a westerly direction reflects the release of pressure in that
324 direction. This is typical of the raising of water pressure and volume in an underlying aquifer above the
325 hydraulic conductivity of the materials, widely reported from proglacially glacitectonized and glacially
326 overridden sediments (Rijsdijk et al. 1999; Le Heron & Etienne 2005; van der Meer et al. 2009; Evans et
327 al. 2012; Roberts et al., 2014). The high pressure gradient developed around the advancing glacier snout
328 responsible for the aggradation of the fan sediment sequence at this site would have been capable of
329 initiating groundwater pressurization and expulsion, together with host aquifer sediments, into the
330 overlying diamictos. The development of the clastic dyke and burst-out structures therefore relates to
331 the period of glacier advance into the depo-centre prior to overriding and drumlinization of the
332 sediments (Fig. 6).

333

334 4.2 Ardillaun Island

335 *Description*

336 The extensive cliffs on the southern and western side of Ardillaun Island (L 627/474; Fig. 1b) provide
337 excellent stratigraphic exposures, up to 12 m high, through a partially eroded drumlin and comprise a 35
338 m long, southwest facing “main section” and a smaller, 10 m long “west section” (Figs. 7 & 8). Bedrock
339 exposures at the eastern end of the island and on the adjacent mainland are orientated 278-198° and
340 297-117° respectively. Two vertical lithofacies logs (Log 1 and 2, Fig. 8) record the sedimentary
341 sequences in the central and eastern parts of the main section respectively. The stratigraphy broadly
342 comprises tabular units, predominantly 1 – 5 m thick, of crudely to well stratified diamictos and coarse
343 gravels, arranged in shallow, westerly to northwesterly dipping clinofolds (Fig. 8), although the upper
344 diamicton at the western end of the section appears more macroscopically massive and contains a
345 larger number of boulders. The nature of the sediments contained within the clinofolds changes
346 relatively abruptly but gradationally in both vertical and horizontal sequences but horizontal erosional

347 contacts also separate the individual tabular units. The dominant horizontally stacked nature of the
348 tabular units is interrupted/truncated at the western end of the main section by a shallow, easterly
349 dipping erosional contact overlain by a further unit of crudely to moderately stratified diamictons and
350 gravels capped by a westerly thinning carapace of massive to fissile diamicton (Fig. 8).

351

352 The sedimentological characteristics of the tabular units exposed at Ardillaun Island are presented in
353 logs 1 and 2 (Fig. 8) and in Figure 7 and are used to classify lithofacies 1-3 (LF 1-3), which occur in
354 interbedded sequences both vertically and horizontally in stacked clinofolds. A further lithofacies (LF 4)
355 occurs as an easterly thickening carapace on the far eastern end of the main section. LF 1 is a laminated
356 to macroscopically massive, relatively clast-poor, matrix-supported diamicton. Lamination is apparent as
357 faint banding and discontinuous partings which locally contain stringers or wisps of sand and fine gravel.
358 Local pockets of laminated sands and silts with limestones (dropstones) form contorted, discontinuous
359 lenses which in some cases are locally interbedded with the gravelly deposits of LF 3 (see below). The
360 laminae in LF 1 reveal that the sediment has been contorted into an open fold in the base of the west
361 section (Fig. 8). LF 2 is a stratified, relatively clast-rich, matrix-supported diamicton in which stratification
362 comprises discontinuous lenses of poorly to moderately well sorted sand and fine gravel. Where these
363 lenses pinch out their margins continue into discontinuous partings in the more massive beds of
364 diamicton. LF 3 comprises localized pockets of matrix-supported to openwork gravels arranged in
365 shallow to relatively steeper and better sorted clinofolds, the latter prompting the classification as
366 gravel foreset beds. Localized pebble to cobble lags are also evident within the better sorted gravel
367 beds. Pockets of poorly sorted to matrix-supported gravels also occasionally form pods and pendant
368 structures whose margins are sharp to diffuse and accordant with open folds or load structures in
369 surrounding diamictons. Discontinuous pockets of laminated and rhythmically bedded fines with
370 dropstones are also included in LF 3. Finally, LF 4 is a fissile and compact, massive, matrix-supported
371 diamicton (Fig. 7, inset photo 4). It lies above a series of faint but laterally extensive and easterly dipping
372 partings developed at the top of underlying beds of LFs 1 and 2, which in contrast dip towards the west.
373 These larger scale partings display the same angle and direction of dip as those of the more densely
374 spaced fissile partings in the overlying Dmm (see stereoplot of fissile partings in Figure 8).

375

376 Clast macrofabrics collected from a variety of locations and from each lithofacies, are predominantly
377 only of moderate strength (i.e. girdle to weakly clustered types) but do reveal a consistent orientation
378 pattern (Fig 8 & Fig. S3). This is a NW-SE and/or NE-SW alignment in both A axes and A/B plane

379 measurements. Clast forms reveal a clear subglacial signature in average roundness (1.88-2.1), number
380 of striated clasts (28-42%) and with shape data plotting close to the till control sample in the RA/C40
381 and average roundness/C40 (Fig. S2) co-variance plots, albeit with variable C40 values. This is a similar
382 trend to clast shape data from north Ballyconneely Bay (see section 4.1) and reflects the abnormally
383 high C40 indices typical of metamorphic grade lithologies. Hence average roundness and C40 co-
384 variance tends to be a more powerful discriminatory tool for differentiating clast transport history. A
385 strong subglacial signature is therefore reflected in low RA values and in the RWR values, which with the
386 exception of one sample at 2% are all zero.

387

388 *Interpretation*

389 The interdigitated and crudely to well stratified diamictos, coarse gravels and matrix-supported gravels
390 exposed at Ardillaun Island are characteristic of sediment gravity flow deposits, especially as they are
391 arranged in shallow clinofolds. Sedimentation in small standing water bodies is recorded by the
392 localized appearance of rhythmically bedded fine-grained deposits and more steeply bedded gravel
393 clinofolds, which are here interpreted as foreset beds. Notwithstanding this evidence for subaqueous
394 sedimentation, the diamictos and matrix-supported gravels are largely only weakly stratified and hence
395 most likely represent cohesive mass flows deposited in shallow water. The discontinuous stratified
396 lenses and partings within diamictos are interpreted as erosional and/or depositional breaks between
397 mass flow emplacement where the stratified sediments represent surface winnowing by traction
398 currents or emplacement of thin turbidites (Nemec & Steel 1984; Postma 1986; Postma et al. 1983;
399 Mulder & Alexander 2001). Based upon these interpretations of lithofacies 1-3, the sedimentary
400 depositional environment in which the majority of the sequence at Ardillaun Island accumulated was
401 likely an immediate ice-proximal depo-centre or shallow angled debris flow-fed subaqueous fan that
402 prograded in a westerly to north-westerly direction from a glacier margin located over southern Mannin
403 Bay (Figs. 1 & 9). Glacier proximity to the depo-centre is indicated by the preservation of significant
404 numbers of striated and sub-rounded clasts. The fan edge was prograded into a shallow subaqueous
405 depositional basin, as indicated by localized foreset beds and rhythmites interdigitated with stacked
406 debris flow diamictos. The largely weakly stratified nature of the diamictos indicates that they were
407 emplaced predominantly by cohesive or hyperconcentrated rather than cohesionless mass flows (cf.
408 Mulder & Alexander 2001). The open folds, load structures and pods and pendants of poorly sorted to
409 matrix-supported gravels visible within the stratigraphic sequence record soft-sediment deformation

410 and slumps folds, likely induced by rapid sediment loading, locally high porewater pressures and mass
411 failure on the surface of the aggrading depo-centre (Rijsdijk & McCarroll 2003).

412
413 The depositional processes responsible for the progradation of lithofacies 1-3 in an ice-marginal fan
414 were terminated by glacier overriding, as evidenced by the emplacement of lithofacies 4, which is
415 interpreted as a subglacial traction till (sensu Evans et al. 2006; Fig. 9). Diagnostic criteria for a traction
416 till origin are the compact, fissile character of the matrix-supported diamicton as well as the strongly
417 accordant orientations of the A axis and A/B plane macrofabrics and partings (fissility), which all indicate
418 a shearing direction from the southeast, even though the fabric strengths are at the girdle end of the
419 subglacial till envelopes (Fig. S3). Glacial shearing from this direction is recorded also by the westerly
420 and west-northwesterly orientated striae that lie immediately beneath the till at the eastern end of
421 Ardillaun Island. The occurrence of southeasterly dipping partings in the upper part of lithofacies 1 and 2
422 immediately beneath lithofacies 4 is indicative of shear deformation in the pre-existing fan deposits.
423 Hence the carapace of massive to fissile diamicton that caps the sequence at Ardillaun Island records the
424 overriding, glacitectonism and streamlining of pre-existing stratified sediments by ice advancing into
425 Mannin Bay from the east or southeast. The progradation of debris flows and foreset beds away from
426 the advancing glacier margin is recorded by the NW-SE and NE-SW orientated clast macrofabrics in the
427 crudely stratified to laminated diamictons and northwesterly dipping foreset bedding. Clast A-axes have
428 been orientated either flow parallel or transverse with a range of fabric strengths from clustered to
429 girdle-like, presumably reflecting varying mass flow viscosities. Corresponding clast A/B planes are
430 predominantly very weakly clustered and strongly girdle-like to isotropic, indicative of low shear stresses
431 and hence unconfined rotation within mass flow matrixes but also common in glacitectonites (cf. Evans
432 et al. 2007).

433

434 4.3 Callow Bridge

435 *Description*

436 A road cut near Callow Bridge (L 643/423; Fig. 1b) provides a 4 m high cliff through a 13 m wide
437 exposure composed of boulder-rich diamicton (Fig. 10). The exposure comprises two matrix-supported
438 diamictons, the lower of which is only poorly exposed up to 1.5 m and appears macroscopically massive.
439 It is separated from the upper massive to highly fissile and relatively boulder-rich diamicton by an
440 undulatory, sharp contact locally marked by a lensate body of sandy material with a pinch and swell
441 geometry (Fig. 10). The basal 30 cm of the upper diamicton also contains a discontinuous horizon or

442 weak pavement containing cobble to boulder size material. This horizon can be traced for more than 10
443 metres along a small drumlin axis-parallel exposure, revealing that the feature continues back into the
444 section face towards the northeast. The boulders that are dispersed through the upper diamicton are
445 clearly uniformly orientated, with their A-axes and A/B planes dipping at shallow angles towards the
446 northeast, and display sub-angular to sub-rounded edges and striated and faceted surfaces (Fig. 10).
447 The numerous anastomosing, sub-horizontal joints that constitute the strong fissility of the upper
448 diamicton are locally associated with small lenses (≤ 10 cm long and 2 cm high) of angular, mono-
449 lithologic and poorly-sorted gravel (Fig. S4).

450
451 Two clast macrofabrics, one from close to the lower contact (CB-F1) and one from above the clast
452 pavement (CB-F2) in the upper diamicton, reveal a consistent NE-SW alignment, especially in the A axis
453 data (Fig. 10). Clast fabric shapes are moderately well clustered for A axes (Fig. S3 left) but range from
454 moderately well clustered to weakly isotropic for A/B planes (Fig. S3 right); sample CB-F1 from the basal
455 and most intensely fissile zone of the diamicton displays strong northeasterly dips for both A axes and
456 A/B planes. The clast form data from both samples in the upper diamicton reveal a strong subglacial
457 signature in average roundness (1.98-2.18) and the number of striated clasts (48-58%). Additionally, the
458 shape data plot close to the till control sample in the RA/C40 and average roundness/C40 (Fig. S2) co-
459 variance plots.

460 461 *Interpretation*

462 The upper diamicton, which forms the core of the Callow Bridge drumlin, is interpreted as a subglacial
463 traction till (sensu Evans et al. 2006) based upon its highly fissile and compact nature, clast form
464 characteristics and clast macrofabrics. Shearing was imparted by ice flowing from the northeast into
465 Ballyconneely Bay. Although the lower diamicton was poorly exposed, it likely forms the lowermost of a
466 stacked sequence of traction tills, separated by a highly attenuated and discontinuous ice-bed
467 separation deposit or canal fill (Eyles et al. 1982; Evans et al. 1995; Piotrowski & Kraus 1997; Piotrowski
468 & Tulaczyk 1999; Boyce & Eyles 2000; Piotrowski et al. 2004). The weakly developed clast pavement
469 likely represents a lag deposit produced by the localized removal of finer grained matrix in the subglacial
470 shear zone, a process associated with the downward migration of the A/B horizon interface in modern
471 subglacial traction tills by Boulton (1996a) and Evans & Hiemstra (2005), possibly aided by meltwater
472 flushing (Boyce & Eyles 2000). The strong fissility, especially in the lower part of the upper diamicton,
473 relates to intense brittle shearing (typical of B horizon subglacial tills; Boulton & Hindmarsh 1987; Benn

474 1995; Hiemstra & Rijdsdijk 2003) and explains the occurrence of small lenses of monolithologic, angular
475 gravel as in situ crushed clasts (Hiemstra & van der Meer 1997) likely liberated from plucked bedrock
476 protuberances.

477

478 **5. Discussion**

479

480 5.1 Controls on drumlin location and depositional origin

481

482 The glacial deposits exposed in the drumlins reported here record ice-marginal and subglacial events
483 associated with the flow of glacier ice from the Connemara mountains across the adjacent coastal
484 lowlands and through Mannin Bay and Ballyconneely Bay. Ice flow directional indicators, such as striae,
485 clast macrofabrics and glacitectonic structures, in addition to drumlin long axis orientations, reveal that
486 ice flow diverged around the Ballyconneely peninsula, entering Mannin Bay from the east or southeast
487 and Ballyconneely Bay from the northeast. At north Ballyconneely Bay and Ardillaun Island, the majority
488 of the observed glacial sediment was delivered not by the subglacial deformation processes most
489 commonly associated with drumlin construction (i.e. Boulton 1987; Hindmarsh 1998a, b; Fowler 2000,
490 2009; King et al. 2007; Schoof 2007; Smith et al. 2007) but by the progradation of subaqueous depo-
491 centres at the grounding lines of glacier margins terminating in water bodies (Powell, 1990). Although a
492 number of previous interpretations of down-glacier dipping stratified sediments in Irish drumlins have
493 invoked the development of subglacial lee-side stratification sequences (e.g. Dardis & Hanvey 1994;
494 Knight 2014), the topographic setting for the stratified sediment assemblages in this study necessitates a
495 more site-specific interpretation; specifically, the locations of the sediment assemblages in coastal
496 lowlands favours the ice-contact subaqueous depositional model proposed by McCabe and Dardis
497 (1989) for the Galway Bay drumlins. Moreover, the existence of till-cored drumlins such as that at
498 Callow Bridge indicates that subaqueous sedimentation was localized on a glacier bed that was
499 otherwise characterized by patchy subglacial traction till deposition and bedrock erosion and scouring.

500

501 Coarse-grained, diamictic debris flow-fed fans have been reported from a variety of glaciated basins
502 where debris-charged glacier snouts have emerged from upland settings and prograded either subaerial
503 and/or subaqueous fans in arcuate assemblages or latero-frontal moraines, fans and ramps (McCabe et
504 al. 1984; Krzyszkowski & Zielinski 2002; Evans et al. 2010). Subaqueous deposition in such settings is
505 likely to be dominated by sediment gravity flows, whose characteristic stratified diamictons will

506 interdigitate with more gravelly deltaic and fan facies as well as finer grained, more distal rhythmites. In
507 an Irish context, the ice-marginal depositional assemblages reported by McCabe and Dardis (1989) from
508 Galway bay, Ó Cofaigh et al. (2011) from the Dingle Peninsula and Evans et al. (2012) from Waterville in
509 County Kerry constitutes a similar stratigraphic record of glaciation in a comparable topographic setting
510 to Mannin Bay and Ballyconneely Bay.

511

512 A modern analogue for the accumulation of the multiple stacked sequences of crudely bedded
513 diamictos at North Ballyconneely Bay and Ardillaun Island, are the mud aprons recognized by
514 Kristensen et al. (2009) in the subaqueous proglacial zones of surging glaciers in Svalbard where
515 sediment is delivered by continuously failing, mobile thrust moraines. Evidence for the operation of syn-
516 depositional glacitectonic deformation of the subaqueous fan is represented by the over-steepened
517 strata exposed in the central sector of the Ballyconneely Bay section. The Svalbard mud aprons are
518 smaller scale examples of diamictic dominated grounding zone wedges formed at the grounding lines of
519 ice streams (e.g., Alley et al., 1989; Licht et al. 1999; Ó Cofaigh et al. 2005; Batchelor and Dowdeswell,
520 2015). Similar depositional processes have been proposed by Evans et al. (2013) for the genesis of
521 multiple stacked diamictos at the margins of palaeo-ice streams of the SW Laurentide Ice Sheet where
522 sediment is delivered to subaqueous proglacial depo-centres by the collapse of till wedges/push
523 moraines during ice advance.

524

525 The localized but significant sediment accumulations represented by the drumlin exposures in this study
526 are conspicuous in a landscape that is otherwise characterized by extensive areally scoured bedrock and
527 the localized emplacement of patches of subglacial traction till. Till cored drumlins represent the
528 streamlining of subglacial traction till layers, which both theory and empirical observation indicate
529 thicken towards glacier and ice sheet margins (Boulton 1996a, b; Evans & Hiemstra 2005; Eyles et al.
530 2011; Evans et al. 2012). Whereas subaerial release of these till layers at the glacier margin produces till
531 wedges or push moraines, their emergence in subaqueous environments leads to the production of
532 interdigitated mass flow diamictos and grounding line fans/wedges. The occurrence of discrete
533 stratified depo-centres within lowland coastal embayments in the study area indicates that glacial
534 sedimentation occurred in a water body located in the embayments during glacier advance. Previous
535 assessments of similar depo-centres, both pre-ice advance (McCabe & Dardis 1989) and deglacial
536 (Thomas & Chiverrell 2006), have entertained the notion of glacioisotatically high sea-level; ice-contact
537 deltas associated with glacier advance and recession into peripheral depressions are commonly used to

538 reconstruct ice sheet palaeoglaciology in coastal settings (e.g. England 1983; England et al. 2000; Evans
539 1990; Ó Cofaigh 1998; Evans et al. 2002; Powell & Cooper 2002; Ó Cofaigh et al. 2003). However, thus
540 far, geological evidence as well as numerically modelled sea level histories for western Ireland indicate
541 that reconstructions of deep water marine conditions around advancing and retreating glacier margins
542 in this region are unlikely (Lambeck 1996; Brookes et al. 2008), and the absence of any in situ marine
543 fauna verifies this modelling output. Consequently, we hypothesise, as have others (e.g. Ó Cofaigh 2011;
544 Evans et al. 2012), that the origins of some of the glacial subaqueous depo-centres around the
545 southern and western Irish coasts were related to glacial processes associated with glacier
546 damming of high to intermediate relief embayments.

547

548 The stratification of drumlins has also been used to support notions of subglacial cavity infilling in areas
549 or corridors of meltwater concentration (Dardis et al. 1984; Hanvey 1987; Dardis & Hanvey 1994;
550 McCabe & Dardis 1994). If the Connemara stratified drumlins originated by such cavity infilling, their
551 locations over coastal embayments indicate that the cavities corresponded with overdeepened portions
552 of the beds of outlet lobes of the Irish Ice Sheet. Consequently we need to entertain the notion of cavity
553 development and enlargement where subglacial drainage channels emerged at former grounding lines
554 (cf. Gorrell & Shaw 1991), which could have developed in either glacial marine or glacial lacustrine settings.
555 Nevertheless, ice sheet marginal lobation due to local topographic controls would likely have initiated
556 lake damming in coastal embayments as the ice sheet advanced from the Connemara mountains
557 towards the continental shelf, which was exposed by glacioeustatic sea-level lowering. The emergence
558 of subglacial drainage tunnels at grounding lines within these localized lake bodies resulted in the
559 progradation of debris-flow fed aprons and subaqueous fans. Debris provision to these depo-centres
560 was most likely from two sources: first, from subglacial sediment advection so that till creep and
561 flowage fed grounding zone wedge/grounding-line fan complexes along the ice margin.; second, from
562 linear concentrations of glacial fluvial sediment, particularly eskers, that accumulated along major
563 meltwater corridors or along former suture zones within the ice sheet, where both supraglacial and
564 subglacial drainage networks converged on the corridors of thinner ice at interlobate zones
565 (Punkari, 1997; Mäkinen 2003; Clark et al. 2012). These marginal sediment wedges or stratified
566 assemblages then became glacial tectonized and subglacially streamlined during glacier overriding. Hence
567 regional drumlin sedimentology reflects the varying degrees of inheritance of pre-existing glacial
568 deposits and suggests that drumlin production relates as much to the position of localised sediment
569 accumulations at the glacier bed and margin (i.e. sticky spots; meltwater tunnel infills; grounding zone

570 wedges; Boulton 1987; Menzies & Brand 2007) as it does to full depth till deformation processes such as
571 instability mechanisms (cf. Fowler 2000; Schoof 2007; Dunlop et al. 2008) within the same drumlin field,
572 as has been acknowledged by Stokes et al. (2013).

573

574 5.2. Drumlin genesis

575

576 Although our study cannot verify the applicability of the instability theory, we can elaborate on the
577 simplified zonation of drumlin types proposed by Stokes et al. (2013) that Type 3 (till cored) drumlins
578 give way down ice to Type 4 (stratified cores with till caps) and then to Type 5 (stratified drumlins). This
579 theoretical zonation appears counter-intuitive in the context of the ice-marginal till thickening model (cf.
580 Boulton 1996a, b; Evans & Hiemstra 2005; Eyles et al. 2011) but is compatible with the increased lateral
581 variability in drumlin composition that would arise from the occurrence of linear assemblages of
582 glacialfluvial (esker) and subaqueous (grounding line) sediments in an otherwise marginal-thickening till
583 sheet (cf. Boyce & Eyles 1991; Evans 1996; Eyles et al. 2011; Evans et al. 2012). Therefore, as a further
584 development of the concepts presented by Boulton (1987) and Stokes et al. (2011, 2013), our prediction
585 is that Types 4 and 5 drumlins should occur in linear assemblages in the outer zones, and more
586 specifically adjacent to the marine margins, of ice sheet beds. The critical control on the formation and
587 location of the linear drumlin assemblages described here is the pre-existence of glacialfluvial (esker) and
588 subaqueous (grounding line fan) sediments which have been overrun. These drumlins are not organised
589 into broad, localised swarms, hence, there is no evidence to support the existence of a widespread
590 mobile deforming bed undergoing instability across the ice sheet bed (Stokes et al., 2013), although it is
591 evident that a deforming layer was in operation (i.e. Callow Bridge drumlin) and that it was likely locally
592 extruded to contribute to the formation of esker ridges and debris flow-fed fans/wedges. Knight (2014)
593 links the genesis of the Connemara drumlins to subglacial sticky spots that evolve through variations in
594 substrate type, meltwater availability and basal shear stress, but does not explore the linear distribution
595 of these features. Furthermore, Knight (2014) invokes leeside cavity formation as a product of
596 perturbation development through instability and secondary feedbacks (i.e. sediment supply and ice
597 creep), although this seems unlikely given the sedimentary continuity between depositional units at
598 Ballyconneely, which demonstrates the ongoing construction of a subaqueous fan complex that is
599 subsequently overrun.

600

601 To produce the distribution of drumlins investigated in this study there are three key control variables, i)
602 laterally restricted sediment delivery to the ice margin via till advection and/or subglacial fluvial
603 processes along well defined corridors; ii) the formation of ice marginal depo-centres controlled by the
604 presence of an ice marginal water body; iii) the advance of ice into and over pre-existing depo-centres to
605 produce streamlined bedforms. Drumlin formation is thus a function of local ice flow dynamics and
606 sediment availability/delivery, and critically in this case, a marginal setting where the combination of
607 these factors acts as the catalyst for the production of local seeding points for drumlin initiation.

608

609 **6. Conclusions**

610 During the last glaciation of western Ireland, glaciers dispersing from the Connemara mountains flowed
611 into the coastal lowlands of Mannin Bay and Ballyconneely Bay, where local topography created lobate
612 ice margins that dammed lakes for short periods prior to ice sheet inundation and advance onto the
613 continental shelf. The progradation of subaqueous depo-centres at the grounding lines of the glacier
614 margins that terminated in these water bodies for short periods during ice sheet advance is recorded in
615 the stratified cores of some drumlins. Contemporaneous glaciectonic disturbance and glacier overriding
616 resulted in the progradation of diamictic, subaqueous debris fans or aprons from continuous sediment
617 flux to the ice margin and the patchy emplacement of a subglacial traction till carapace associated with
618 drumlinization of the subaqueous depo-centres. We propose that the localized occurrence of stratified
619 drumlin cores on a glacier bed that was predominantly characterized by till-cored drumlin formation and
620 bedrock erosion/scouring can be explained by the former existence of linear assemblages of subglacial
621 drainage channels/eskers and associated grounding line deposits. Hence we predict that stratified cored
622 and and till capped (Type 4) and stratified cored (Type 5) drumlins should occur in linear assemblages
623 around the outer, marine margins of drumlinized ice sheet beds.

624

625 **Acknowledgements**

626 Chris Orton, Durham University drafted the figures for this paper. Constructive comments from Emrys
627 Phillips and John Hiemstra helped us to clarify the details of this paper.

628

629 **References**

- 630 Alley RB, Blankenship DD, Rooney ST, Bentley CR, 1989. Sedimentation beneath ice shelves – the view
631 from ice stream B. *Marine Geology* 85, 101-120.
- 632 Ballantyne CK, Stone JO, McCarroll D, 2008. Dimensions and chronology of the last ice sheet in Western
633 Ireland. *Quaternary Science Reviews* 27, 185-200.
- 634 Batchelor, C.L., Dowdeswell, J.A., 2015. Ice-sheet grounding-zone wedges (GZWs) on high-latitude
635 continental margins. *Marine Geology* 363, 65-92.

- 636 Benn DI, 1994. Fabric shape and the interpretation of sedimentary fabric data. *Journal of Sedimentary*
637 *Research A* 64: 910–915.
- 638 Benn DI, 1995. Fabric signature of till deformation, Breiðamerkurjökull, Iceland. *Sedimentology* 42: 735–
639 747.
- 640 Benn DI, 1996. Subglacial and subaqueous processes near a glacier grounding line: sedimentological
641 evidence from a former ice-dammed lake, Achnasheen, Scotland. *Boreas* 25: 23–36.
- 642 Benn DI, 2004b. Clast morphology. In *A Practical Guide to the Study of Glacial Sediments*, Evans DJA,
643 Benn DI (eds.) Arnold: London; 77–92.
- 644 Benn DI, Ballantyne CK, 1994. Reconstructing the transport history of glacial sediments: a new
645 approach based on the co-variance of clast form indices. *Sedimentary Geology* 91: 215–227.
- 646 Benn DI, Evans DJA, 1996. The interpretation and classification of subglacially deformed materials.
647 *Quaternary Science Reviews* 15: 23–52.
- 648 Benn DI, Evans DJA, Phillips ER, Hiemstra JF, Walden J, Hoey TB, 2004. The research project — a case
649 study of Quaternary glacial sediments. In *A Practical Guide to the Study of Glacial Sediments*,
650 Evans DJA, Benn DI (eds.) Arnold: London; 209–234.
- 651 Boulton GS, 1987. A theory of drumlin formation by subglacial deformation. In *Drumlin Symposium*,
652 Rose J, Menzies J. (eds.) Balkema: Rotterdam; 25–80.
- 653 Boulton GS, 1996a. Theory of glacial erosion, transport and deposition as a consequence of subglacial
654 sediment deformation. *Journal of Glaciology* 42: 43–62.
- 655 Boulton GS, 1996b. The origin of till sequences by subglacial sediment deformation beneath mid-latitude
656 ice sheets. *Annals of Glaciology* 22: 75–84.
- 657 Boulton GS, Hindmarsh RCA, 1987. Sediment deformation beneath glaciers: rheology and geological
658 consequences. *Journal of Geophysical Research* 92: 9059–9082.
- 659 Boyce JI, Eyles N, 1991. Drumlins carved by deforming till streams below the Laurentide ice sheet.
660 *Geology* 19: 787–790.
- 661 Boyce JI, Eyles N, 2000. Architectural element analysis applied to glacial deposits: internal geometry of a
662 late Pleistocene till sheet, Ontario, Canada. *Geological Society of America Bulletin* 112: 98–118.
- 663 Brookes AJ, Bradley SL, Edwards RJ, 2008. Postglacial relative sea level observations from Ireland
664 and their role in glacial rebound modelling. *Journal of Quaternary Science* 23: 175–192.
- 665 Carr SJ 2004. Micro scale features and structures. In, Evans DJA & Benn DI (eds.), *A Practical Guide to the*
666 *Study of Glacial Sediments*. Arnold, London, 115–144.
- 667 Charlesworth JK, 1929. The glacial retreat in Iar Connacht. *Proceedings of the Royal Irish Academy*,
668 39B, 95–106.
- 669 Cheel RJ, Rust BR, 1982. Coarse grained facies of glacio-marine deposits near Ottawa, Canada. In
670 *Research in Glaciofluvial and Glaciolacustrine Systems*, Davidson-Arnott R, Nickling W, Fahey
671 BD (eds.) Geobooks: Norwich, UK; 279–295.
- 672 Clark CD, Hughes ALC, Greenwood SL, Jordan C, Sejrup HP, 2012. Pattern and timing of retreat of the last
673 British-Irish Ice Sheet. *Quaternary Science Reviews* 44, 112–146.
- 674 Dardis GF, 1985. Till facies associations in drumlins and some implications for their mode of formation.
675 *Geografiska Annaler* 67A: 13–22.
- 676 Dardis GF, 1987. Sedimentology of late Pleistocene drumlins in south-central Ulster, Northern Ireland.
677 In, Menzies J & Rose J (eds.), *Drumlin Symposium*. Balkema, Rotterdam, 215–224.
- 678 Dardis GF, Hanvey PM 1994. Sedimentation in a drumlin lee-side wave cavity, northwest Ireland.
679 *Sedimentary Geology* 91, 97–114.
- 680 Dardis GF, McCabe AM, 1983. Facies of subglacial channel sedimentation in late-Pleistocene drumlins,
681 Northern Ireland. *Boreas* 12: 263–278.
- 682 Dardis GF, McCabe AM, 1987. Subglacial sheetwash and debris flow deposits in late Pleistocene

683 drumlins, Northern Ireland. In, Menzies J & Rose J (eds.), Drumlin Symposium. Balkema,
684 Rotterdam, 224-240.

685 Dardis GF, McCabe AM, Mitchell WI, 1984. Characteristics and origins of leeside stratification sequences
686 in Late Pleistocene drumlins, Northern Ireland. *Earth Surface Processes and Landforms* 9: 409-
687 424.

688 Dunlop P, Clark CD, Hindmarsh RCA, 2008. Bed ribbing instability explanation: testing a numerical model
689 of ribbed moraine formation arising from the coupled flow of ice and subglacial sediment.
690 *Journal of Geophysical Research* 113: (F3), F03005. <http://dx.doi.org/10.1029/2007JF000954>.

691 England J, 1983. Isostatic adjustments in a full glacial sea. *Canadian Journal of Earth Sciences* 20: 895-
692 917.

693 England J, Smith IR, Evans DJA, 2000. The last glaciation of east-central Ellesmere Island, Nunavut: ice
694 dynamics, deglacial chronology, and sea level change. *Canadian Journal of Earth Sciences* 37:
695 1355-1371.

696 Evans DJA, 1990. The last glaciation and relative sea level history of NW Ellesmere Island, Canadian
697 high arctic. *Journal of Quaternary Science* 5, 67–82.

698 Evans DJA, 1996. A possible origin for a megafluting complex on the southern Alberta prairies,
699 Canada. *Zeitschrift fur Geomorphologie Supplementband* 106, 125–148.

700 Evans DJA, 2010. Controlled moraine development and debris transport pathways in polythermal
701 plateau icefields: examples from Tungnafellsjökull, Iceland. *Earth Surface Processes and*
702 *Landforms* 35: 1430–1444.

703 Evans DJA, Benn DI, 2004. Facies description and the logging of sedimentary exposures. In *A Practical*
704 *Guide to the Study of Glacial Sediments*, Evans DJA, Benn DI (eds). Arnold: London; 11–51.

705 Evans DJA, Hiemstra JF, 2005. Till deposition by glacier submarginal, incremental thickening. *Earth*
706 *Surface Processes and Landforms* 30: 1633–1662.

707 Evans DJA, Hiemstra JF, Ó Cofaigh C, 2007. An assessment of clast macrofabrics in glacial sediments
708 based on A/B plane data. *Geografiska Annaler* 89A: 103–120.

709 Evans DJA, Hiemstra JF, Ó Cofaigh C, 2012. Stratigraphic architecture and sedimentology of a Late
710 Pleistocene subaqueous moraine complex, southwest Ireland. *Journal of Quaternary Science* 27:
711 51-63.

712 Evans DJA, Owen LA, Roberts D, 1995. Stratigraphy and sedimentology of Devensian (Dimlington Stadial)
713 glacial deposits, east Yorkshire, England. *Journal of Quaternary Science* 10: 241–265.

714 Evans DJA, Rea BR, Hansom JD, Whalley WB, 2002. The geomorphology and style of plateau icefield
715 glaciation in a fjord terrain, Troms–Finnmark, north Norway. *Journal of Quaternary Science* 17,
716 221–239.

717 Evans DJA, Phillips ER, Hiemstra JF, Auton CA, 2006. Subglacial till: formation, sedimentary
718 characteristics and classification. *Earth-Science Reviews* 78: 115–176.

719 Evans DJA, Rother H, Hyatt OM, Shulmeister J, 2013. The glacial sedimentology and geomorphological
720 evolution of an outwash head/moraine-dammed lake, South Island, New Zealand. *Sedimentary*
721 *Geology* 284-285: 45-75.

722 Evans DJA, Shulmeister J, Hyatt OM, 2010. Sedimentology of latero-frontal moraines and fans on
723 the west coast of South Island, New Zealand. *Quaternary Science Reviews* 29: 3790–3811.

724 Eyles N, Eyles C, Menzies J, Boyce J, 2011. End moraine construction by incremental till deposition
725 below the Laurentide Ice Sheet: Southern Ontario, Canada. *Boreas* 40: 92-104.

726 Eyles N, Eyles CH, Miall AD, 1983. Lithofacies types and vertical profile models: an alternative approach
727 to the description and environmental interpretation of glacial diamict and diamictite sequences.
728 *Sedimentology* 30: 393–410.

729 Eyles N, Sladen JA, Gilroy S, 1982. A depositional model for stratigraphic complexes and facies
730 superimposition in lodgement tills. *Boreas* 11: 317–333.

731 Fowler AC, 2000. An instability mechanism for drumlin formation. In *Deformation of Glacial Materials*,
732 Maltman A, Hambrey MJ, Hubbard B (eds.) Geological Society: London, Special Publication 176:
733 307-319.

734 Fowler AC, 2009. Instability modelling of drumlin formation incorporating leeside cavity growth.
735 *Proceedings of the Royal Society of London, Series A* 465: 2681-2702.

736 Gorrell G, Shaw J, 1991. Deposition in an esker, bead and fan complex, Lanark, Ontario, Canada.
737 *Sedimentary Geology* 72: 285–314.

738 Greenwood SL, Clark CD, 2008. Subglacial bedforms of the Irish Ice Sheet. *Journal of Maps* 2008, 332-
739 357.

740 Greenwood SL, Clark CD, 2009a. Reconstructing the last Irish Ice Sheet 1: changing flow geometries and
741 ice flow dynamics deciphered from the glacial landform record. *Quaternary Science Reviews* 28,
742 3085-3100.

743 Greenwood & Clark 2009b. Reconstructing the last Irish Ice Sheet 2: a geomorphologically-driven model
744 of ice sheet growth, retreat and dynamics. *Quaternary Science Reviews* 28, 3103-3123.

745 Hanvey PM, 1987. Sedimentology of lee-side stratification sequences in late-Pleistocene drumlins,
746 north-west Ireland. In *Drumlin Symposium*, Menzies J, Rose J (eds.) Balkema: Rotterdam; 241-
747 253.

748 Hicock SR, Goff JR, Lian OB, Little EC, 1996. On the interpretation of subglacial till fabric. *Journal of*
749 *Sedimentary Research* 66: 928–934.

750 Hiemstra JF, Rijdsdijk KF, 2003. Observing artificially induced strain: implications for subglacial
751 deformation. *Journal of Quaternary Science* 18: 373-383.

752 Hiemstra JF, van der Meer JJM, 1997. Pore water controlled grain fracturing as an indicator for subglacial
753 shearing in tills. *Journal of Glaciology* 43: 446-454.

754 Hindmarsh RCA, 1998a. Drumlinization and drumlin forming instabilities: viscous till mechanisms.
755 *Journal of Glaciology* 44: 293–314.

756 Hindmarsh RCA, 1998b. The stability of a viscous till sheet coupled with ice flow, considered at
757 wavelengths less than the ice thickness. *Journal of Glaciology* 44: 285–292.

758 King EC, Woodward J, Smith AM. 2007. Seismic and radar observations of subglacial bed forms beneath
759 the onset zone of Rutford Ice Stream, Antarctica. *Journal of Glaciology* 53: 665–672.

760 King EL, Hafliðason H, Sejrup H-P, Lovlie R. 1998. Glacigenic debris flows on the North Sea trough-
761 mouth fan during ice stream maxima. *Marine Geology* 152, 217-246.

762 Knight J, 2014. Subglacial hydrology and drumlin sediments in Connemara, western Ireland. *Geografiska*
763 *Annaler* 96, 403-415.

764 Kristensen L, Benn DI, Hormes A, et al. 2009. Mud aprons in front of Svalbard surge moraines: evidence
765 of subglacial deforming layers or proglacial glaciotectonics? *Geomorphology* 111: 206–221.

766 Krzyszkowski D, Zielinski T, 2002. The Pleistocene end moraine fans: controls on their sedimentation
767 and location. *Sedimentary Geology* 149, 73–92.

768 Lachniet MS, Larson GJ, Strasser JC, Lawson DE, Evenson EB, Alley RB, 1999. Microstructures of
769 glacial debris flow deposits, Matanuska Glacier, Alaska. In *Glacial Processes Past and Present*,
770 Mickelson DM, Attig JW (eds.) Geological Society of America: Boulder, Special Paper 337; 45-57.

771 Lachniet MS, Larson GJ, Lawson DE, Evenson EB, Alley RB, 2001. Microstructures of sediment flow
772 deposits and subglacial sediments: a comparison. *Boreas* 30, 254-262.

773 Lambeck K, 1996. Glaciation and sea level change for Ireland and the Irish Sea since late
774 Devensian/Midlandian time. *Journal of the Geological Society of London* 153: 853–872.

775 Le Heron DP, Etienne JL. 2005. A complex subglacial clastic dyke swarm, Solheimajökull, southern
776 Iceland. *Sedimentary Geology* 181: 25–37.

777 Li D, Yi C, Ma B, Wang P, Ma C, Cheng G, 2006. Fabric analysis of till clasts in the upper Urumqi River,
778 Tian Shan, China. *Quaternary International* 154–155: 19–25.

779 Licht, K.J., Dunbar, N.W., Andrews, J.T., Jennings, A.E. 1999. Distinguishing subglacial till and glacial
780 marine diamictons in the western Ross Sea, Antarctica: implications for last glacial maximum
781 grounding line. *Geological Society of America Bulletin* 111, 91-103.

782 Linton DL 1963. The forms of glacial erosion. *Transactions of the Institute of British Geographers* 33, 1-
783 28.

784 Lukas S, Benn DI, Boston CM, Brook M, Coray S, Evans DJA, Graf A, Kellerer-Pirklbauer A, Kirkbride MP,
785 Krabbendam M, Lovell H, Machiedo M, Mills SC, Nye K, Reinardy BTI, Ross FH, Signer M, 2013.
786 Clast shape analysis and clast transport paths in glacial environments: A critical review of
787 methods and the role of lithology. *Earth-Science Reviews* 121: 96–116.

788 Mäkinen J, 2003. Time-transgressive deposits of repeated depositional sequences within interlobate
789 glaciofluvial (esker) sediments in Koylio, SW Finland. *Sedimentology* 50, 327-360.

790 McCabe AM, Dardis GF, 1989. Sedimentology and depositional setting of late Pleistocene drumlins,
791 Galway Bay, western Ireland. *Journal of Sedimentary Petrology* 59: 944-959.

792 McCabe AM, Dardis GF, 1994. Glaciotectonically induced water-throughflow structures in a Late
793 Pleistocene drumlin, Kanrawer, County Galway, western Ireland. *Sedimentary Geology* 91: 173-
794 190.

795 McCabe AM, Dardis GF, Hanvey PM. 1984. Sedimentology of a Late Pleistocene submarine–moraine
796 complex, County Down, Northern Ireland. *Journal of Sedimentary Petrology* 54: 716–730.

797 McCabe AM, Dardis GF, Hanvey PM. 1987. Sedimentation at the margins of a late Pleistocene ice lobe
798 terminating in shallow marine environments, Dundalk Bay, eastern Ireland. *Sedimentology* 34:
799 473–493.

800 Menzies J, 2000. Micromorphological analyses of microfabrics and microstructures indicative of
801 deformation processes in glacial sediments. In *Deformation of Glacial Materials*, Maltman AJ,
802 Hubbard B, Hambrey MJ (eds.) Geological Society: London, Special Publication 176; 245–257.

803 Menzies J, Brand U, 2007. The internal sediment architecture of a drumlin, Port Byron, New York State,
804 USA. *Quaternary Science Reviews* 26: 322-335.

805 Mulder T, Alexander J. 2001. The physical character of subaqueous sedimentary density flows and their
806 deposits. *Sedimentology* 48: 269–299.

807 Nemeč W, Steel RJ. 1984. Alluvial and coastal conglomerates: their significant features and some
808 comments on gravelly mass-flow deposits. In *Sedimentology of Gravels and Conglomerates*,
809 Koster EH, Steel RJ (eds). *Memoir 10. Canadian Society of Petroleum Geologists: Calgary*; 1–31.

810 Ó Cofaigh C, 1998. Geomorphic and sedimentary signatures of early Holocene deglaciation in high arctic
811 fiords, Ellesmere Island, Canada: implications for deglacial ice dynamics and thermal regime.
812 *Canadian Journal of Earth Sciences* 35: 437-452.

813 Ó Cofaigh C, Evans DJA, Hiemstra JF. 2008. Till sedimentology and stratigraphy on the Dingle Peninsula,
814 south-west Ireland: implications for Late Quaternary regional ice flow patterns. *Proceedings of*
815 *the Geologists' Association* 119: 137–152.

816 Ó Cofaigh C, Evans DJA, Hiemstra J. 2011. Formation of a stratified subglacial ‘till’ assemblage by ice-
817 marginal thrusting and glacier overriding. *Boreas* 40: 1–14.

818 Ó Cofaigh C, Taylor J, Dowdeswell JA, Pudsey CJ, 2003. Palaeo-ice streams, trough- mouth fans and high
819 latitude continental slope sedimentation. *Boreas* 32: 37-55.

820 Ó Cofaigh, C., Dowdeswell, J. A., Allen, C. S., Hiemstra, J.F., Pudsey, C.J., Evans, J., Evans, D.J.A. 2005.
821 Flow dynamics and till genesis associated with a marine-based Antarctic palaeo-ice stream.
822 *Quaternary Science Reviews* 24, 709–740.

823 Ó Cofaigh C, Dunlop P Benetti S. 2012. Marine geophysical evidence for Late Pleistocene ice
824 sheet extent and recession off northwest *Ireland*. *Quaternary Science Reviews* 44, 147–159.

825 Orme AR 1967. Drumlins and the Weichsel glaciation of Connemara. *Irish Geography* 5, 262–274.

826 Phillips ER 2006. Micromorphology of a debris flow deposit: evidence of basal shearing, hydrofracturing,
827 liquefaction and rotational deformation during emplacement. *Quaternary Science Reviews* 25,
828 720–738.

829 Piotrowski JA, Kraus AM, 1997. Response of sediment to ice sheet loading in northwestern Germany:
830 effective stresses and glacier bed stability. *Journal of Glaciology* 43: 495–502.

831 Piotrowski JA, Tulaczyk S, 1999. Subglacial conditions under the last ice sheet in northwest Germany:
832 ice-bed separation and enhanced basal sliding? *Quaternary Science Reviews* 18: 737–751.

833 Piotrowski JA, Larsen NJ, Junge FW, 2004. Reflections on soft subglacial beds as a mosaic of deforming
834 and stable spots. *Quaternary Science Reviews* 23: 993–1000.

835 Postma G. 1986. Classification for sediment-gravity flow deposits based on flow conditions during
836 sedimentation. *Geology* 14: 291–294.

837 Postma G, Roep TB, Ruegg GHJ. 1983. Sandy gravelly mass flow deposits in an ice-marginal lake (Saalian,
838 Leuvenumsche Beek Valley, Veluwe, The Netherlands) with emphasis on plug flow deposits.
839 *Sedimentary Geology* 34: 59–82.

840 Powell RD. 1990. Glacimarine processes at grounding-line fans and their growth to ice-contact deltas. In
841 *Glacimarine Environments: Processes and Sediments*, Dowdeswell JA, Scourse JD (eds). Special
842 Publication 53. Geological Society: London; 53–73.

843 Powell RD 2003. Subaquatic landsystems: fjords. In: Evans, D.J.A. (Ed.), *Glacial Landsystems*. Arnold,
844 London, 313–347.

845 Powell RD, Cooper JM. 2002. A glacial sequence stratigraphic model for temperate, glaciated
846 continental shelves. In: Dowdeswell, J.A., Ó Cofaigh, C. (Eds.), *Glacier-Influenced Sedimentation
847 on High-Latitude Continental Margins*. Geological Society Special Publication 203, London, pp.
848 215–244.

849 Punkari M 1997. Glacial and glaciofluvial deposits in the interlobate areas of the Scandinavian ice sheet.
850 *Quaternary Science Reviews* 16, 741–753.

851 Rea BR, Evans DJA 1996. Landscapes of aerial scouring in NW Scotland. *Scottish Geographical Magazine*
852 112, 47–50.

853 Rijdsdijk KF, Owen G, Warren WP, 1999. Clastic dykes in overconsolidated tills: evidence for subglacial
854 hydrofracturing at Killiney Bay, eastern Ireland. *Sedimentary Geology* 129: 111–126.

855 Rust BR, Romanelli R. 1975. Late Quaternary subaqueous outwash deposits near Ottawa, Canada. In
856 *Glaciofluvial and Glaciolacustrine Sedimentation*, Jopling AV, McDonald BC (eds). Special
857 Publication 23. SEPM: Tulsa, OK; 177–192.

858 Schoof C, 2007. Pressure-dependent viscosity and interfacial instability in coupled ice-sediment flow.
859 *Journal of Fluid Mechanics* 570: 227–252.

860 Shaw J, 1983. Drumlin formation related to inverted meltwater erosional marks. *Journal of Glaciology*
861 29: 461–479.

862 Shaw J, Kvill D, 1984. A glaciofluvial origin for drumlins of the Livingstone Lake area, Saskatchewan.
863 *Canadian Journal of Earth Sciences* 12: 1426–1440.

864 Shaw J, Kvill D, Rains RB, 1989. Drumlins and catastrophic subglacial floods. *Sedimentary Geology* 62:
865 177–202.

866 Shaw J, Faragini D, Kvill DR, Rains RB, 2000. The Athabasca fluting field, Alberta, Canada: implications for
867 the formation of large scale fluting (erosional lineations). *Quaternary Science Reviews* 19: 959–
868 980.

869 Smith, M.J. and Knight, J., 2011. Palaeoglaciology of the last Irish Ice Sheet reconstructed from striae
870 evidence. *Quaternary Science Reviews* 30, 147–160.

871 Smith AM, Murray T, Nicholls KW, Makinson K, Aðalgeirsdóttir G, Behar AE, Vaughan DG, 2007. Rapid

872 erosion, drumlin formation, and changing hydrology beneath an Antarctic ice stream. *Geology*
873 35: 127-130.

874 Spedding N, Evans DJA, 2002. Sediments and landforms at Kvíárjökull, southeast Iceland: a reappraisal of
875 the glaciated valley landsystem. *Sedimentary Geology* 149: 21–42.

876 Stokes CR, Fowler AC, Clark CD, Hindmarsh RCA, Spagnolo M, 2013. The instability theory of drumlin
877 formation and its explanation of their varied composition and internal structure. *Quaternary*
878 *Science Reviews* 62: 77-96.

879 Stokes CR, Spagnolo M, Clark CD, 2011. The composition and internal structure of drumlins: complexity,
880 commonality, and implications for a unifying theory of their formation. *Earth Science Reviews*
881 107: 398-422.

882 Sugden DE & John BS 1976. *Glaciers and Landscape*. Arnold, London.

883 Synge, F.M., 1968. The glaciation of west Mayo. *Irish Geography* 5, 372–386.

884 Thomas GSP, Chiverrell RC. 2006. A model of subaqueous sedimentation at the margin of the Late
885 Midlandian Irish Ice Sheet, Connemara, Ireland, and its implications for regionally high isostatic
886 sea levels. *Quaternary Science Reviews* 25: 2868–2893.

887 van der Meer JJM, 1993. Microscopic evidence of subglacial deformation. *Quaternary Science Reviews*
888 12: 553-587.

889 van der Meer JJM, Kjær KH, Kruger J, 2009. Under pressure: clastic dykes in glacial settings. *Quaternary*
890 *Science Reviews* 28: 708–720.

891 Vorren TO, Laberg JS, 1997. Trough-mouth fans: palaeoclimate and ice sheet monitors. *Quaternary*
892 *Science Reviews* 16: 865-881.

893 Warren, W.P., 1992. Drumlin orientation and the pattern of glaciation in Ireland. *Sveriges Geologiska*
894 *Undersökning* 81, 359–366.

895

896

897 **Figure captions**

898 Figure 1: Location maps of the study area in Connemara, County Galway: a) regional physiography and
899 key locational information, with study area outlined by black box; b) topography and study site
900 locations in the area outlined in Figure 1a by the black box. The areas of closely spaced lakes
901 represent areal scour terrain with very thin glacial sediment cover; c) Google Earth image of
902 the study area and adjacent terrain, showing drumlins as well vegetated ovoid forms distributed
903 over the extensive bedrock exposures of the areal scour terrain; d) Google Earth image of the
904 Callow Bridge and adjacent inland drumlins.

905

906 Figure 2: Overviews of the glacially streamlined terrain in the study area: a) view southwards across the
907 streamlined bedrock of inner Mannin Bay with the sediment cored drumlin of Ardillaun Island in
908 the middle distance; b) view across striated and abraded bedrock bumps at Earawalla Point
909 towards the sediment-cored drumlin of Mutton Island; c) view westward across the streamlined
910 bedrock of Ballyconneely Bay to the exposure through the sediment core of the north
911 Ballyconneely Bay drumlin.

912

913 Figure3: The north Ballyconneely Bay drumlin section: a) section sketch showing major lithofacies and
914 sedimentary architecture (inset photograph of western end of section shows over-steepened
915 bedding architecture and true dip of overall sequence, made available at a three-dimensional

916 exposure due to a cliff indentation); b vertical profile logs 1 – 4 , showing major lithofacies, clast
917 fabric stereonets and clast form data.

918

919 Figure 4: Panel of sediment types from N Ballyconneely Bay: a) matrix-supported diamicton with
920 localized stratified sediment lens; b) prominent stratification represented by interbedded
921 gravelly diamictons and stratified sands and gravels arranged in shallow angled clinofolds; c)
922 rhythmically bedded silts and fine sands with dropstones lying in conformable sequence with
923 stratified, matrix-supported diamictons; d) details of scoured and horizontal, conformable
924 contacts within the interbedded gravelly diamictons and stratified sands and gravels in panel
925 “b”; e) interbedded gravelly diamictons and stratified sands and gravels, showing abrupt and
926 gradational contacts.

927

928 Figure 5: Thin section photographs of North Ballyconneely Bay sediments: a) Thin section B’Conn 5 –
929 crudely stratified diamict which includes reworked intraclasts of sorted silt/clay, occasional
930 dropstones, evidence for compression and contortion, secondary fluidisation, rotation and
931 necking. Plasmic fabrics include skelsepic and masepic fabrics and variable domain textures. b)
932 Thin section B’Conn 2 - interlaminated sands, silts and clays with dropstones. Evidence of
933 water escape and secondary structures including minor open folds, normal and reverse faulting,
934 low angle shear faults, minor boudinage and extension of laminae. Plasmic fabrics include
935 kinking fabrics within clay laminae

936 Figure 6: Diagrammatic reconstruction of the evolution of the sedimentary sequence at North
937 Ballyconneely Bay (upper panels) and sketch maps of associated palaeoglaciological
938 reconstructions. Early phase A involved intermittent sub-marginal till wedge development and
939 subaqueous failure of the resulting push moraine to produce long run-out sediment gravity
940 flows (yellow). Pulses of subglacial meltwater, relating to periods of ice-bed separation and
941 temporary cessation of subglacial deformation, are recorded in packages of foreset-bedded
942 gravels (orange). During late phase A there was a switch to predominantly subglacial glacialfluvial
943 processes, which resulted in the progradation of a subaqueous grounding line fan and ultimately
944 the advance of the glacier snout into the depo-centre, resulting in its glacitectonic deformation,
945 hydrofracture development and then further subaqueous fan progradation. Phase B involved ice
946 overriding and the drumlinization of the subaqueous depo-centre, during which glacitectonite
947 (red) and subglacial traction till (green) were developed.

948

949 Figure 7: The Ardillaun Island main section (photograph overviews 1-4 and main sediment types i – iii).
950 The upper photo-montage shows localized details of the sedimentary architecture and character
951 of lithofacies. Photographs i-iii show the main sediment types: i) laminated and macroscopically
952 massive, matrix-supported diamictons; ii) foreset beds comprising matrix-supported to
953 openwork gravels and overlying laminated sands and silts with lonestones (dropstones); iii)
954 clinofolds comprising stratified, relatively clast-rich, matrix-supported diamicton with
955 discontinuous lenses of poorly to moderately well sorted sand and fine gravel.

956

957 Figure 8: The Ardillaun Island sections, showing section sketches of the major sedimentary structures in
958 the main section (upper three panels), the west section, vertical profile logs 1 and 2, and the
959 details and locations of clast macrofabric and clast shape data.

960

961 Figure 9: Diagrammatic reconstruction of the evolution of the sedimentary sequence at Ardillaun
962 Island. See Figure 6 for palaeoglaciological reconstruction. Phase A involved intermittent sub-
963 marginal till wedge development and subaqueous failure of the resulting push moraine to
964 produce long run-out sediment gravity flows (yellow). Pulses of subglacial meltwater, relating to
965 periods of ice-bed separation and temporary cessation of subglacial deformation, are recorded
966 in packages of foreset-bedded gravels (orange). Phase B involved ice overriding, drumlinization
967 of the subaqueous depo-centre and the production of a subglacial traction till carapace (green).

968

969 Figure 10: The Callow Bridge drumlin section showing major lithofacies and sedimentary architecture
970 on an annotated photograph montage, inset photographs of lithofacies details and clast fabric
971 stereonet and clast form data.

972

973

974 **Supporting information**

975

976 Figure S1: Clast form control sample data from a previous study in glaciated terrain with
977 similar metamorphic grade lithologies in New Zealand (from Evans et al. 2010).

978

979 Figure S2: Clast form co-variance plots for the sediments sampled in this study: a)
980 RA/C40; b) average roundness/C40. For comparison with the control sample data presented in
981 Supplementary Figure 1. As RWR values were zero for all but one sample, an RWR/C40 plot is
982 not included here.

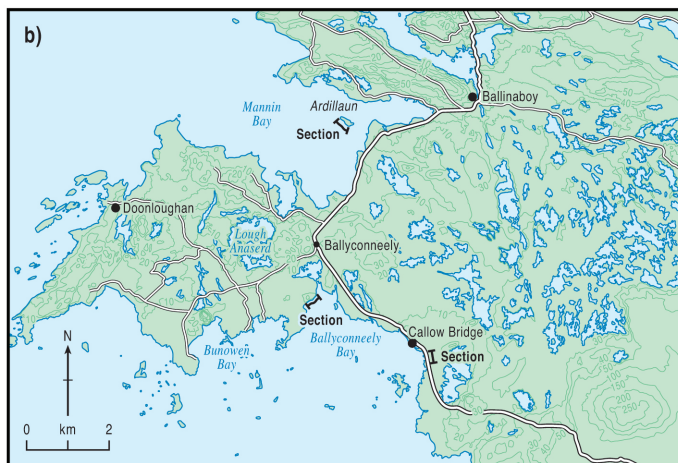
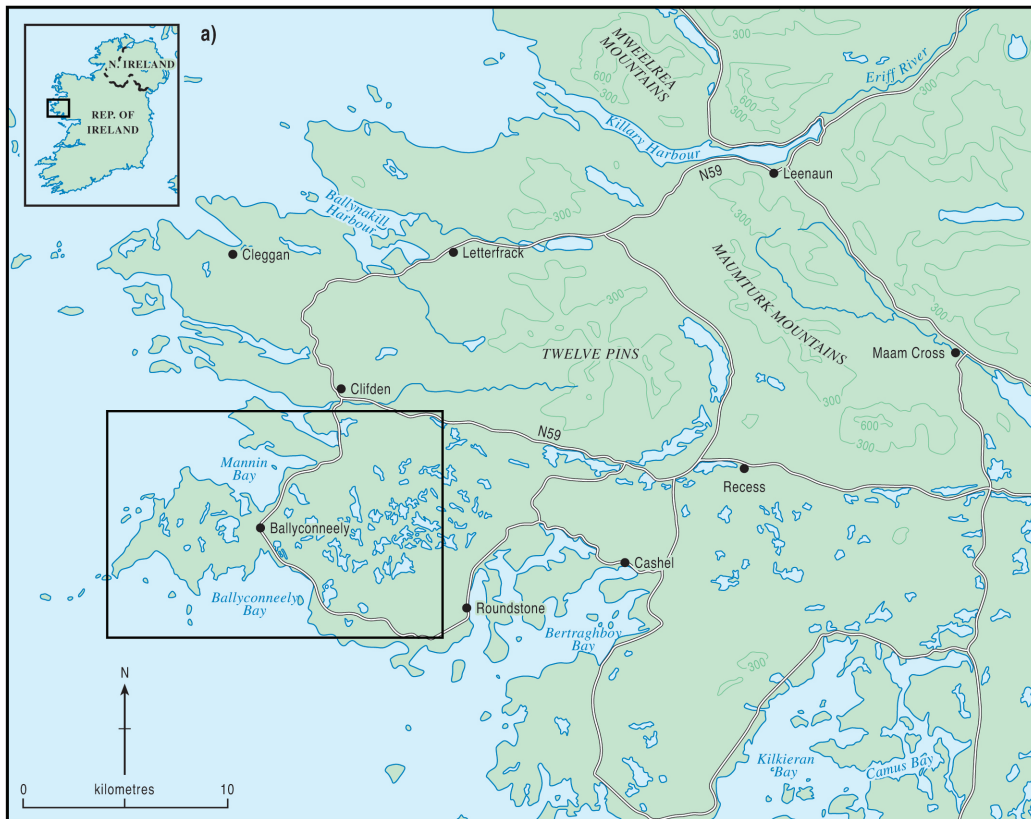
983

984 Figure S3: Clast macrofabric shape ternary plots for the sediments sampled in this
985 study: a) A-axis data; b) A/B plane data. Envelopes for samples of known origin are based upon
986 previous studies (Evans & Hiemstra 2005; Evans et al. 2007; Benn & Evans 2010).

987

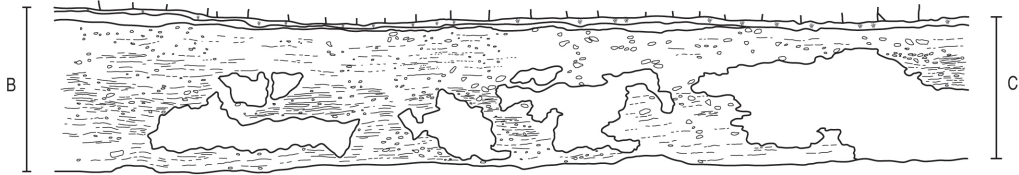
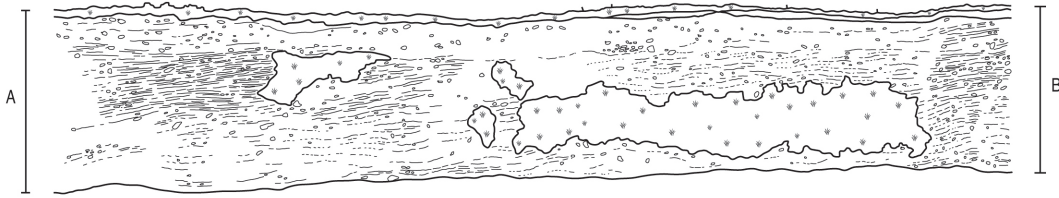
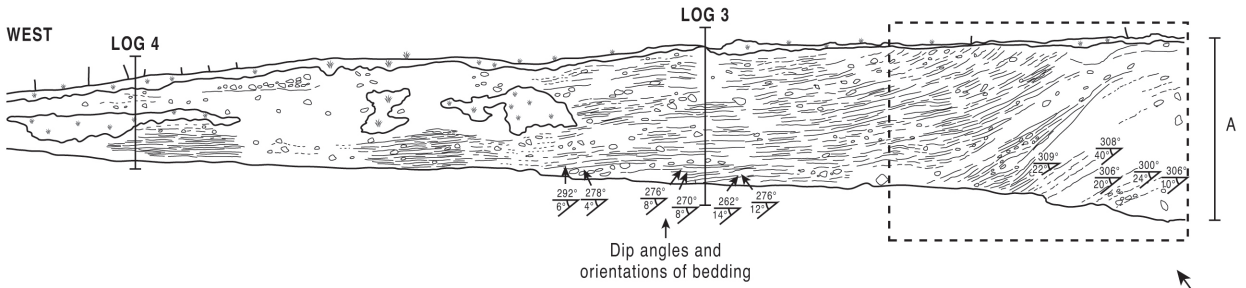
988 Figure S4: Detailed photograph of the upper diamicton at Callow Bridge, showing
989 numerous anastomosing, sub-horizontal joints that constitute the strong fissility.

990

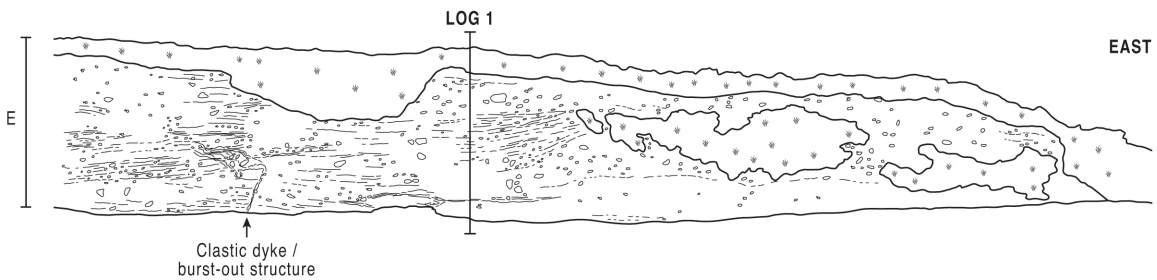
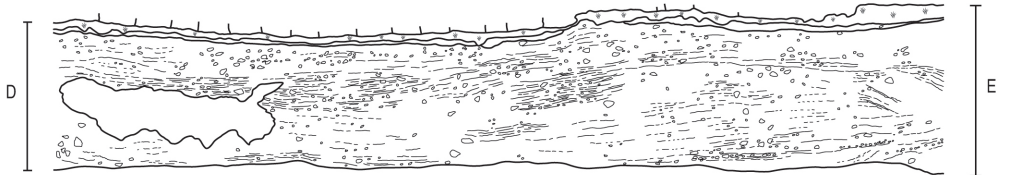
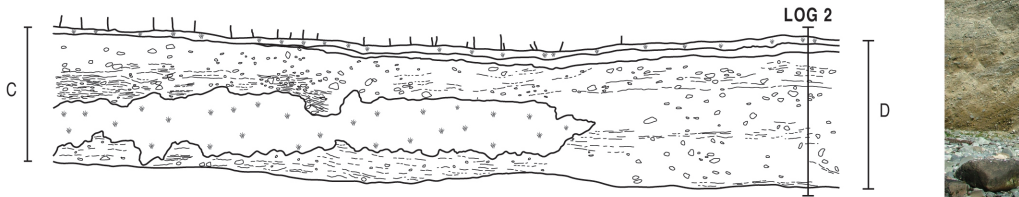




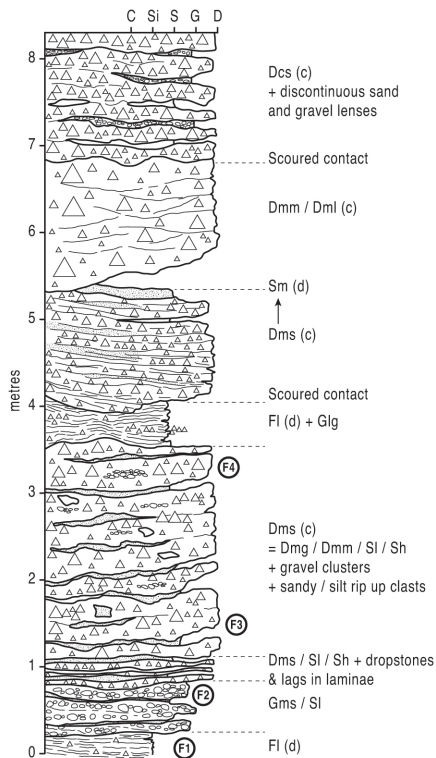
North Ballyconneely Bay



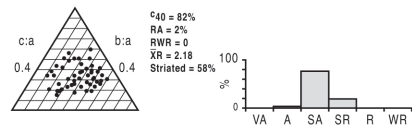
Ballyconneely 3



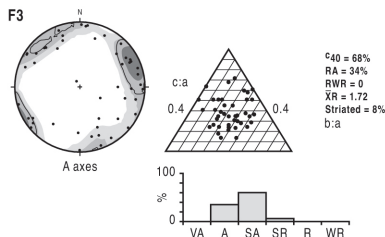
North Ballyconneely Bay
Log 3



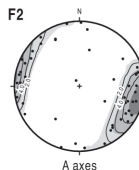
F4



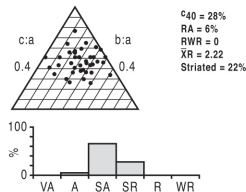
F3



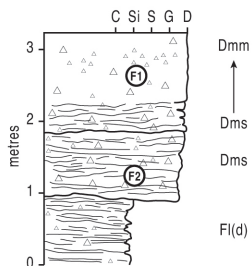
F2



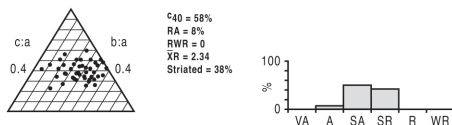
F1



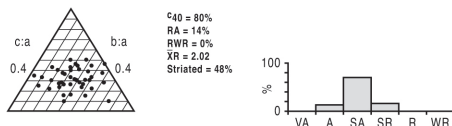
North Ballyconneely Bay
Log 4



F1

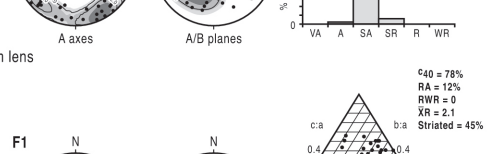
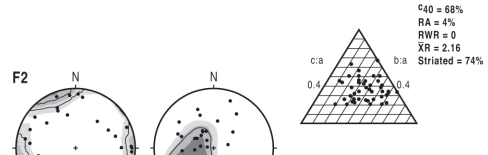
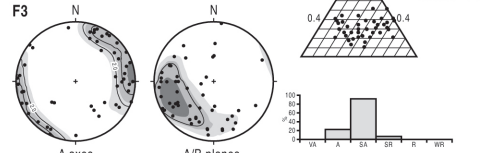
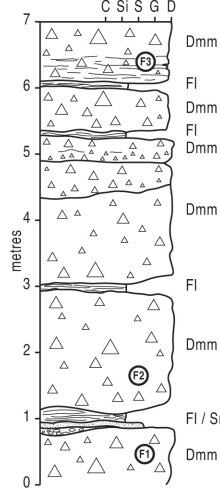


F2

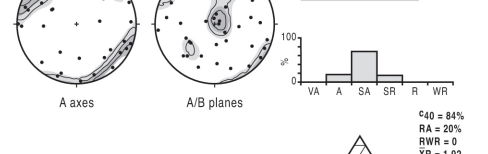
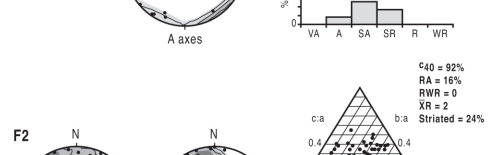
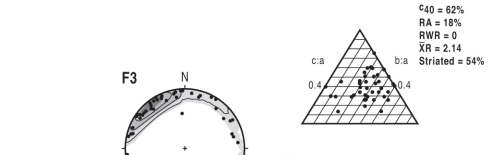
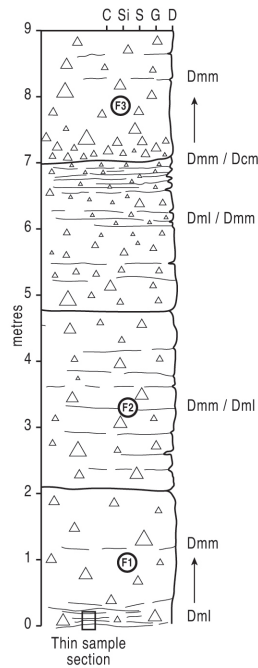




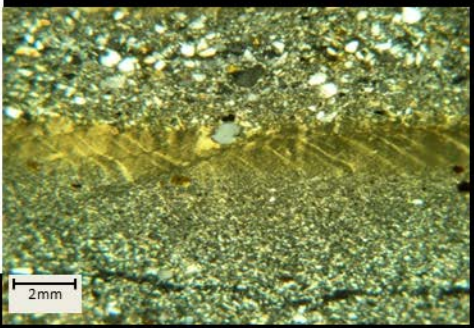
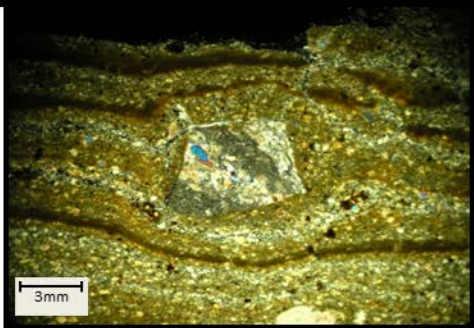
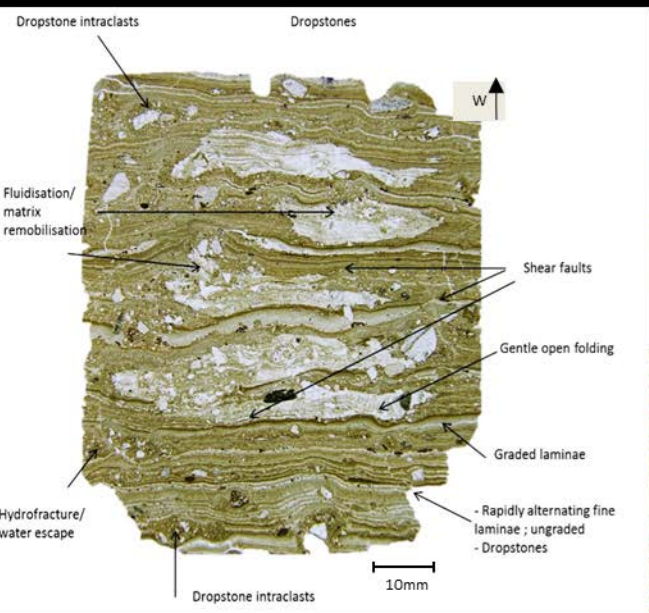
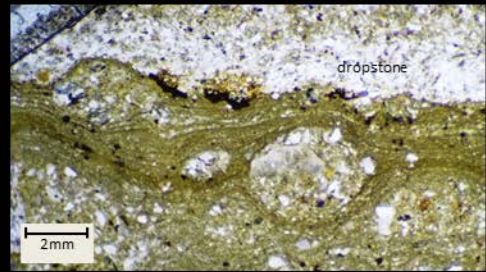
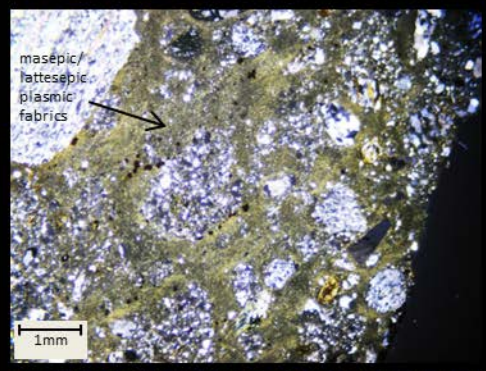
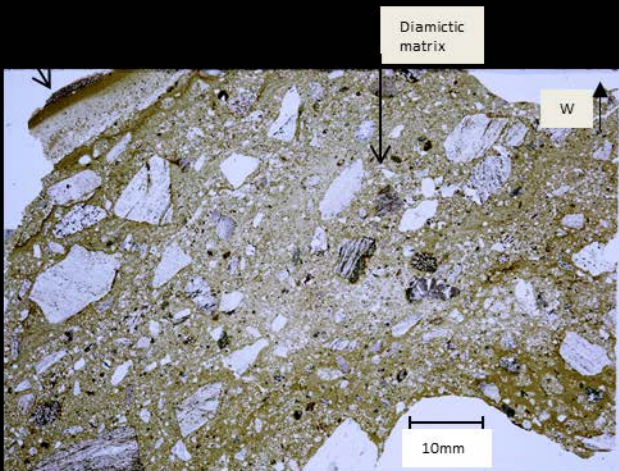
North Ballyconneely Bay Log 1



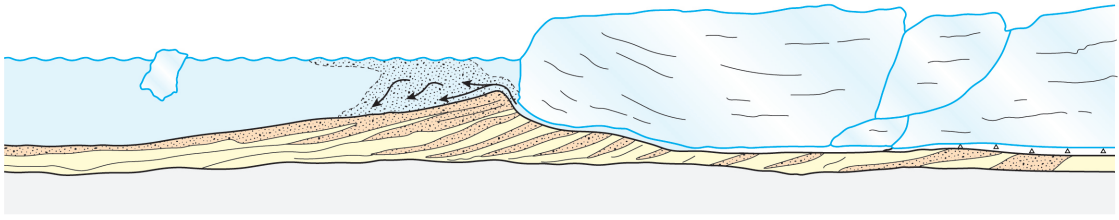
North Ballyconneely Bay Log 2



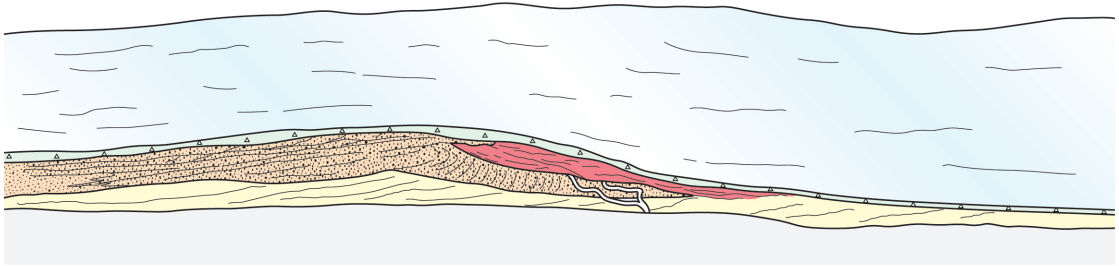
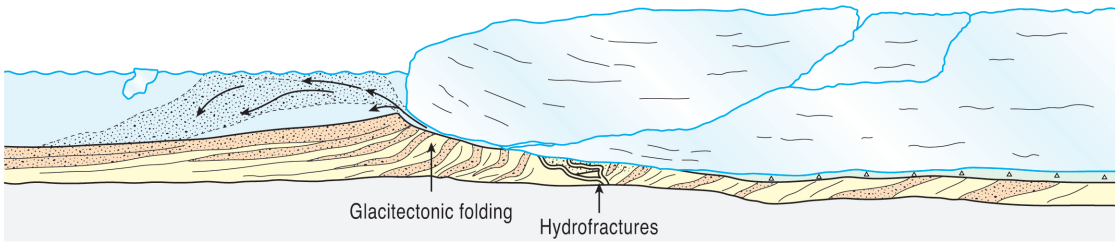




NORTH BALLYCONNEELY BAY
(depositional scenario)

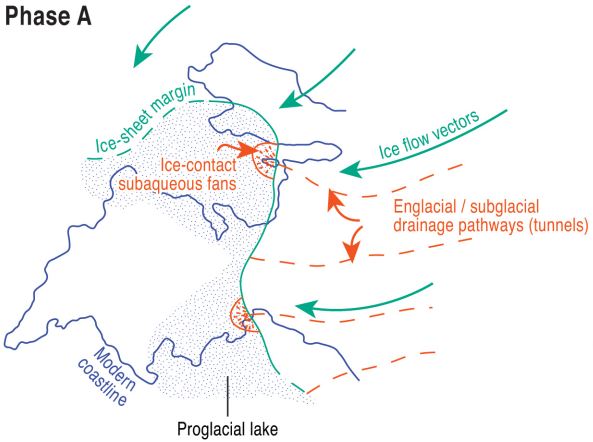


Phase A

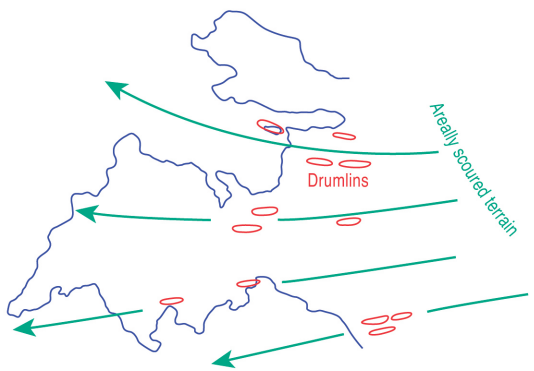


Phase B

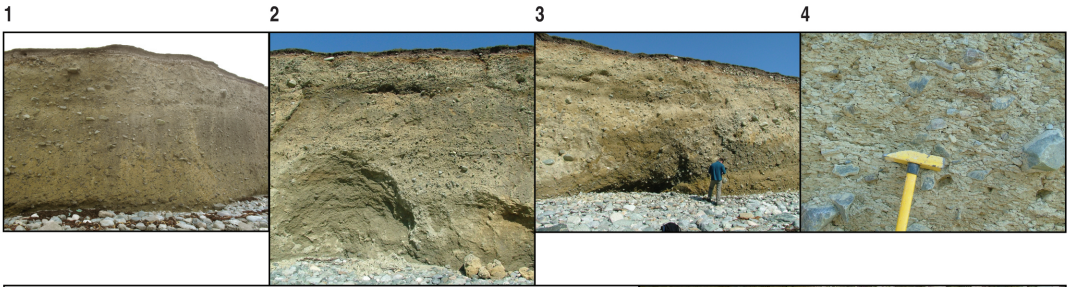
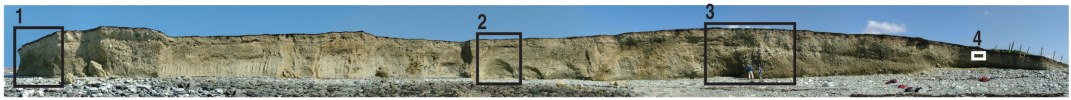
Phase A



Phase B



Ardillaun (main section)



Ardillaun (main section)



Photo 1 (Figure 10a)

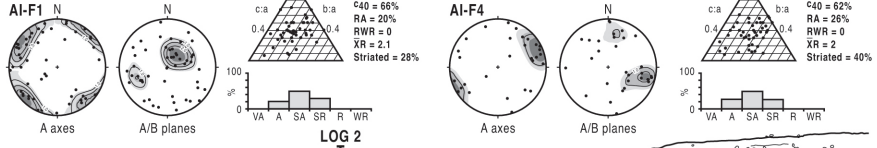


Photo 2 (Figure 10a)

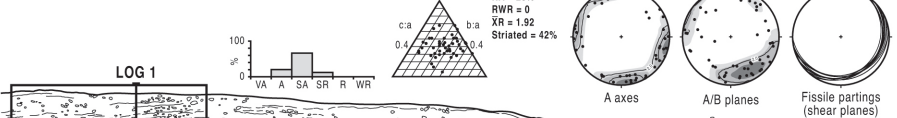
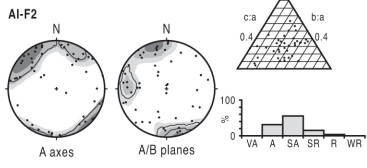
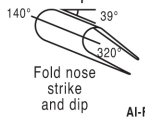
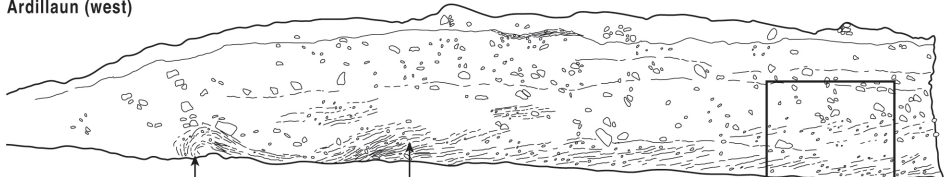
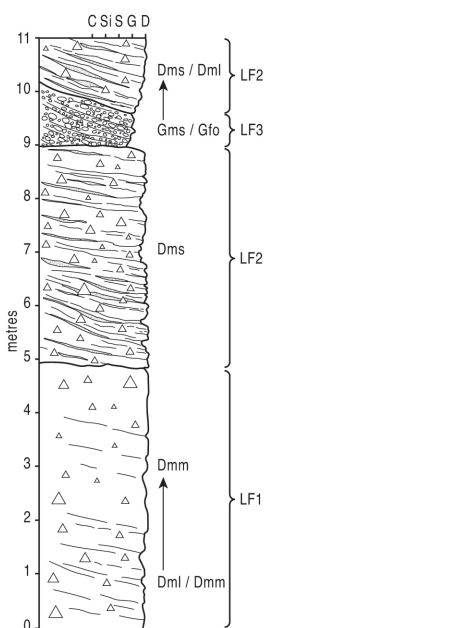


Photo 3 (Figure 10a)

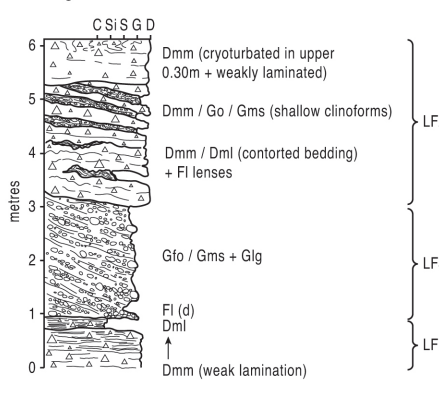
Ardillaun (west)



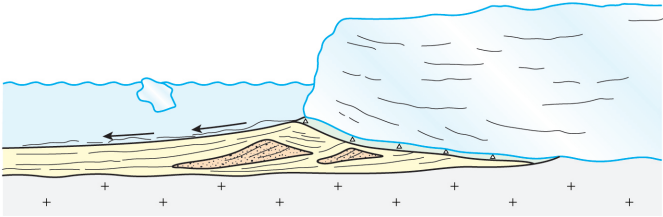
Ardillaun Island Log 2



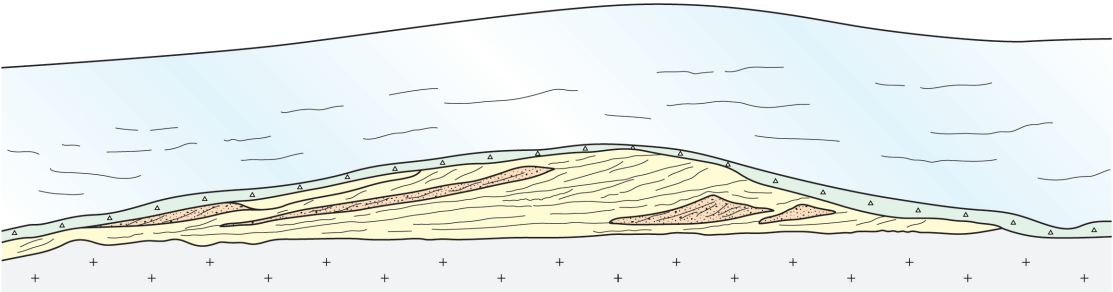
Ardillaun Island Log 1



ARDILLAUN ISLAND
(depositional scenario)

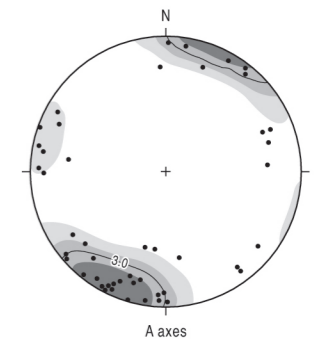
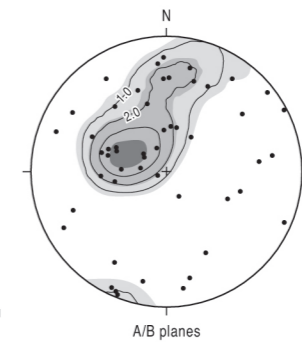
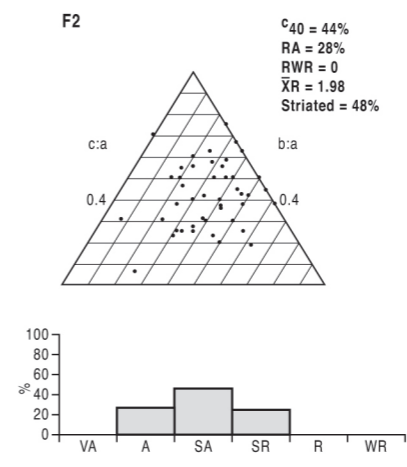
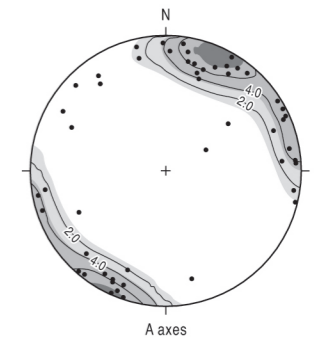
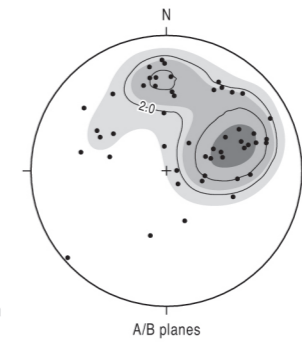
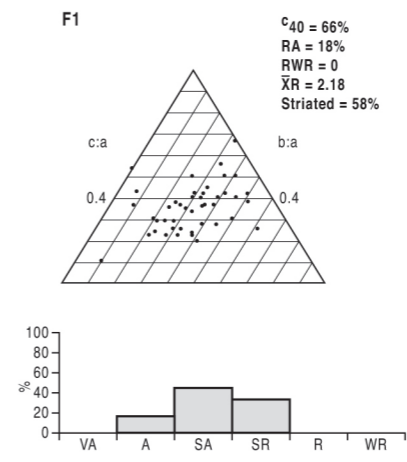


Phase A

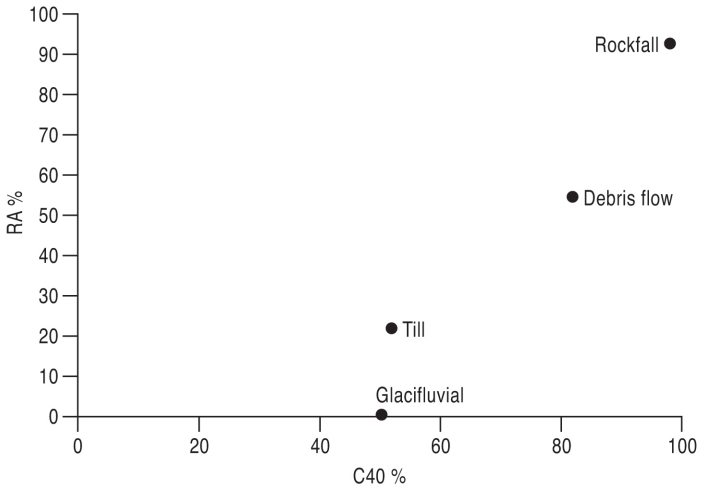


Phase B

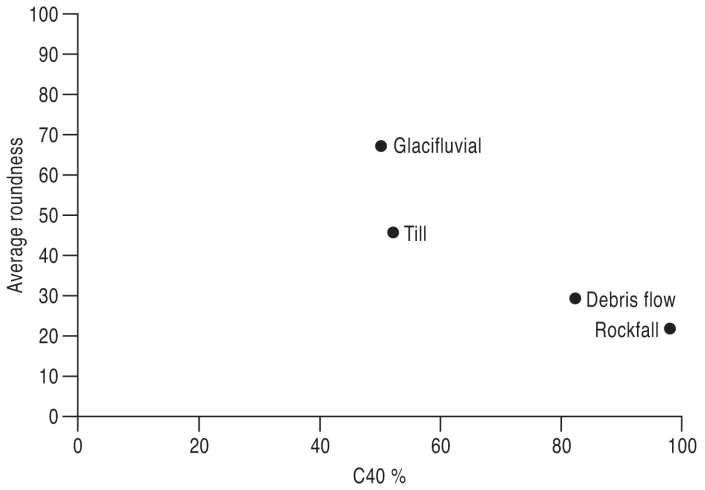
Callow Bridge



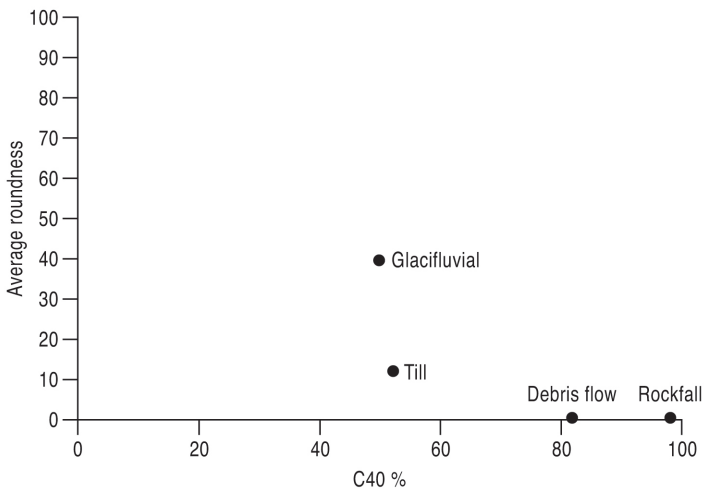
Clast form co-variance



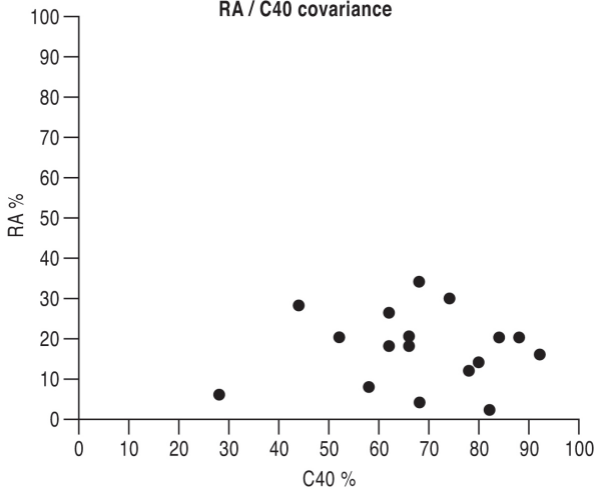
Co-variance (average roundness & C40)



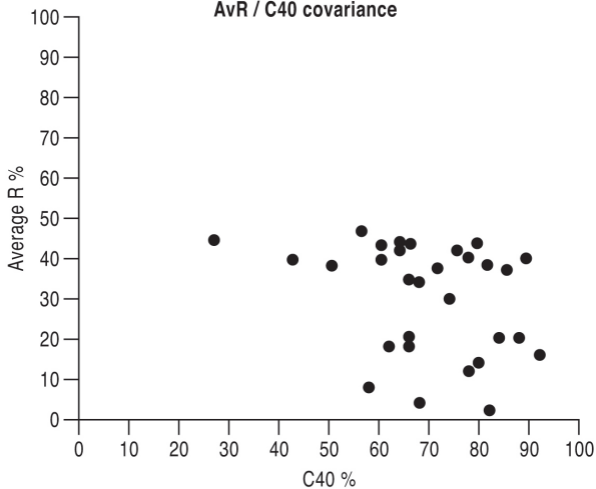
Co-variance (RWR & C40)



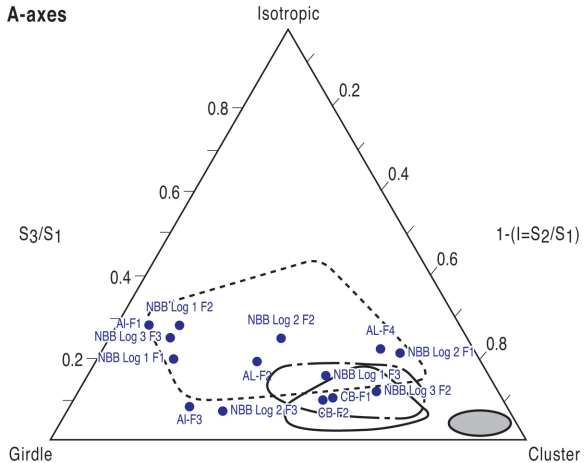
RA / C40 covariance



AvR / C40 covariance

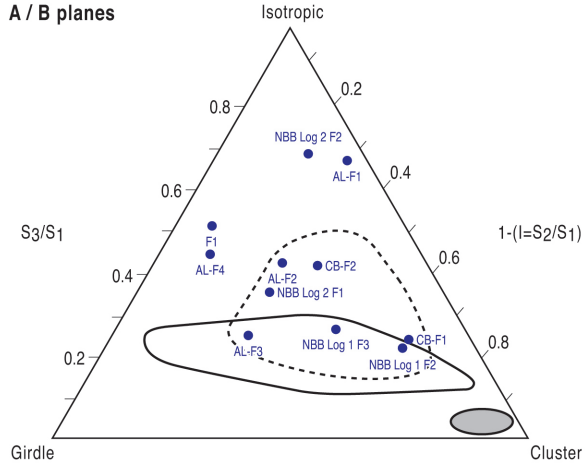


A-axes



- Breiðamerkurjökull upper till (Benn & Evans, 1996)
- _____ Breiðamerkurjökull lower till (Benn & Evans, 1996)
- - - - - Glaciotectonite (Benn & Evans, 1996)
- Lodged clasts (Evans and Hiemstra 2005)

A / B planes



- _____ Glaciotectonite continuum (Evans *et al* 1999 and Hiemstra *et al* 2007)
- Subglacial till (Evans and Hiemstra 2005)
- Lodged clasts (Evans and Hiemstra 2005)

